CHARACTERIZATION OF WOUND MONITORING SYSTEMS USED TO QUANTIFY AND LOCATE PLUTONIUM CONTAMINATION

A Thesis

by

PAUL JAMES DIMMERLING

Submitted to the Office of Graduate Studies of
Texas A&M University
in partial fulfillment of the requirements for the degree of

MASTER OF SCIENCE

December 2007

Major Subject: Health Physics

CHARACTERIZATION OF WOUND MONITORING SYSTEMS USED TO QUANTIFY AND LOCATE PLUTONIUM CONTAMINATION

A Thesis

by

PAUL JAMES DIMMERLING

Submitted to the Office of Graduate Studies of
Texas A&M University
in partial fulfillment of the requirements for the degree of

MASTER OF SCIENCE

Approved by:

Chair of Committee,	Leslie A. Braby
Committee Members,	John W. Poston Sr.
	Michael Walker
Head of Department,	Raymond J. Juzaitis

December 2007

Major Subject: Health Physics

ABSTRACT

Characterization of Wound Monitoring Systems Used to Quantify and Locate Plutonium Contamination. (December 2007)

Paul James Dimmerling, B.S., The Ohio State University

Chair of Advisory Committee: Dr. Leslie A. Braby

When an accident involving the possibility of a plutonium contaminated wound occurs, the contamination is often quantified using sodium iodide (NaI(Tl)) and high purity germanium (HPGe) detection systems. The NaI(Tl) system is used to quantify the amount of contamination, while HPGe is used to gauge the depth of contamination in the wound. Assessment of plutonium contaminated wounds is difficult due to the low-energy and yield of the uranium L-shell x rays used for the measurement, which can be effected by source distance, shape, and tissue attenuation. These effects on wound counting systems used at Los Alamos National Laboratory (LANL) were characterized experimentally using common source shapes (disk, point, and line) and acrylic plastic as a tissue substitute. Experiments were conducted to characterize detector responses as a function of tissue attenuation, source distance, and source depth in tissue. The computer code MCNP5 was used to model both systems for wound counting and better examine angular displacement of a line source in tissue.

The NaI(Tl) detector response was characterized using absolute detector efficiency for all experimental measurements. Measurements showed that the NaI(Tl)

system is significantly effected by the source to detector position and depth in tissue. Characterization of the HPGe detection system was done utilizing the peak-to-peak ratio from the two low-energy x rays. HPGe peak-to-peak ratios were not affected by source to detector distance, but showed an increased response to source depth in tissue. MCNP results suggested that small incident angles from the plane of the detector face can cause significant effects on the response of both detectors. In summary, the response of both systems showed dependence on source geometry and depth of contamination in tissue. Correction values and uncertainties were determined based on these dependencies.

DEDICATION

To my wife family and friends. Without your love, help, and encouragement this would have never been possible.

ACKNOWLEDGEMENTS

I would like to thank Jeff Whicker for his support and guidance throughout my research. Without him I would have not received the funding or support to do this research at Los Alamos National Laboratory.

I would also like to acknowledge my committee chair, Dr. Leslie A. Braby, and my committee members, Dr. John W Poston Sr., Dr. Michael Walker, and Dr. Jeffrey Whicker, for their guidance and support throughout the course of this research.

Thanks also go to my friends and colleagues and the nuclear engineering department faculty and staff for making my time at Texas A&M University a great experience. I also want to extend my gratitude to the Los Alamos National Lab Radiation Protection Group, which provided the instruments, funding, and technical support form this research. I would also like to thank Dr. Murray E. Moore for the uses of his lab space and his support throughout this research.

Finally, thanks to my mother and father for their encouragement and to my wife for her patience and love.

NOMENCLATURE

ALI	Annual Limit on Intake
Bq	becquerel
DAC	Derived Air Concentration
DOE	Department of Energy
HPGe	High Purity Germanium Detector
HV	High Voltage
ICRP	International Commission of Radiological Protection
ICRU	International Commission on Radiation Units and Measurements
keV	kiloelectron Volt
LANL	Los Alamos National Laboratory
MCA	Multichannel Analyzer
MCB	Multichannel Buffer
MDA	Minimum Detectable Activity
MPA	Minimum Peak Area
MPBB	Maximum Permissible Body Burden
NaI(Tl)	Sodium Iodide Thallium Doped Detector
nCi	nanocurie
NIST	National Institute of Standards and Technology
Pu	Plutonium
^{239}Pu	Plutonium 239

ROI	Region of Interest

TABLE OF CONTENTS

Page

LIST OF FIGURES

Page

LIST OF TABLES

CHAPTER I

INTRODUCTION

Many Department of Energy (DOE) facilities are charged with ensuring the dependability of the United States nuclear weapons stockpile. Making sure the nuclear deterrent is ready and operational requires research into both warhead reliability and warhead replacement. Research in warhead reliability focuses on making certain that older weapons will work, if needed, and warhead replacement requires modifying or replacing multiple parts of the existing weapons to ensure their operation. Both of these initiatives center on the plutonium pit, which is the fissile core of the nuclear weapon. Thus, there are many different chemical and mechanical operations and experiments that involve ^{239}Pu, in which workers can be exposed to the ^{239}Pu in its various physical and chemical forms.

Workers can be exposed to the radioactive emissions of ^{239}Pu through internal and external forms of radiation exposure. Worker exposure to external forms of radiation results from x rays, gamma rays and neutrons being emitted from the ^{239}Pu, other plutonium isotopes, and their respective radioactive progeny. In the worst case, if too much plutonium is placed in one spot it can form a critical mass, which would release large amounts of radiation in the form of prompt gamma rays and neutrons. This external exposure to high levels of gamma and neutron radiation can result in a large dose to nearby occupants rather quickly. Internal exposure to plutonium occurs when it is inhaled, ingested, or injected into the body. All three routes of entry can occur when processing and machining of ^{239}Pu, but this paper focuses on the detection and quantification of injected ^{239}Pu through accidental wounds.

This thesis follows the style of *Health Physics Journal*.

PLUTONIUM CHARACTERISTICS

Physical Characteristics

Plutonium (Pu) has an atomic number of 94, is a heavy metal, and is a solid at room temperature, and has a silvery-white appearance. The main isotope of interest in nuclear weapons by weight is ^{239}Pu which has a half life of 24,065 years (ICRP 1983). ^{239}Pu is not generally found in nature and has been synthetically produced in nuclear reactors since the 1940's. ^{239}Pu decays by emitting 5.105, 5.143, 5.156 MeV alpha particles, which transition the nucleus to a uranium atom.(ICRP 1983) Many times the resultant uranium atom has an unstable electron configuration at which point it will emit x rays when the electron shells reconfigure to become stable. The emitted x rays are considered to be characteristic of the ^{239}Pu decay process and are called uranium L shell x rays. For this study, the x rays emitted with energies of 13.60, 17.06, and 20.30 keV with yields of 1.48, 2.09, and 0.49 respectively were of interest (ICRP 1983).

Chemical Characteristics

Chemical forms of plutonium can vary widely, but the primary forms used in nuclear weapons production include plutonium nitrate, plutonium metal, and PuO_2. Plutonium nitrate is the chemical form that is common in many radiochemistry labs, and is used for analysis of samples for mass spectroscopy and is an intermediate chemical form for the conversion of plutonium oxide to metal. The metal form of plutonium is commonly used in many facilities around LANL for experiments and making plutonium pits. PuO_2 is also a very common chemical form of plutonium found in plutonium facilities. Knowing the chemical form of the plutonium in a wound is important because it determines the biokinetics in the body and ultimately the magnitude of the dose received (Guilmette and Durbin 2003).

Biological Kinetics

The three routes of intake that can result in an internal exposure to plutonium are inhalation, ingestion, and injection. For this study, injection is the form of intake of concern. No guidance document provides values of the annuals limit on intake (ALI) for injected plutonium but there is information available for inhalation and ingestion in the 10 CFR 820 & 835 document. The ALI and DAC are tabulated in table 1 below for the three absorption classes F (fast), M (moderate), and S (slow) as defined in the ICRP 78 documents for inhalation radionuclide is only dependent on the f1 value (ICRP 1997). Table 2 below is the tabulated type or f1 value for different plutonium compounds with respect to both inhalation and ingestion (10 CFR 820 & 835).

Table 1: 10 CFR 820 & 835 ALI and DAC limits for plutonium.

Absorption	ALI	DAC	Limiting
Type	(Bq)	(Bq/m^3)	Tissue
F	N/A	N/A	N/A
M	240	0.1	Bone Surfaces
S	4800	2	Bone Surfaces

Table 2: ICRP 78 plutonium classification.

Intake	Type	f1	Chemical Compounds
Inhalation	M	5.0E-04	Unspecified Compounds
Inhalation	S	1.0E-05	Insoluble Oxides
Ingestion		5.0E-04	Unspecified Compounds
Ingestion		1.0E-05	Insoluble Oxides
Ingestion		1.0E-04	Nitrates

Unlike inhalation and ingestion, injection allows the material to enter the body in such a way that it can go directly into the blood. The circulatory system can then transport the plutonium to other tissues and organs in the body. A mathematically-based biokinetic model for the prediction of systemic transport of radionuclides has been developed and is described in ICRP Publication 67 (ICRP 1987). Figure 1 is a graphical representation of this model from the ICRP-67. The primary organs for plutonium

retention in this model are the liver, cortical bone surfaces, and trabecular bone surfaces, as outlined in ICRP 78 (ICRP 1997).

Depending on the amount and chemical form of the plutonium in the wound, it will leach into the blood and be transported to various tissues with the amounts and rates depending on the solubility of plutonium an ultimately result in dose to the body (Guilmette and Durbin 2003). The doses resulting from wounds can be significant, certainly above regulatory limits, and require medical intervention to lower the committed dose equivalent (Carbaugh et al. 1989, Bailey et al. 2003). Therefore it is important to accurately quantify the amount of plutonium in the wound to determine which medical treatment, if any, to pursue.

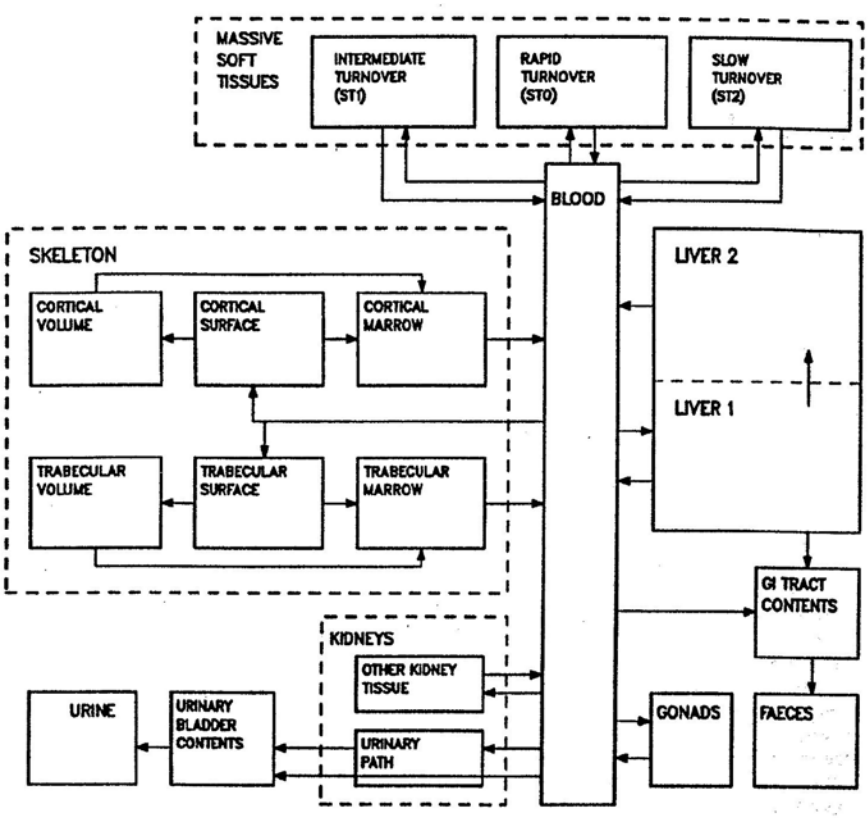

Figure 1: Biokinetic model for systemically incorporated radionuclides. Figure taken from ICRP Publication 67 (ICRP 1987).

PLUTONIUM CONTAMINATED WOUNDS

History of Contaminated-Plutonium Wounds

Los Alamos National Laboratory (LANL) and other institutions have had incidents in the past where someone was injured while working with ^{239}Pu. Many of these incidents have occurred during the machining of plutonium parts or while working in gloved boxes on plutonium experiments. These injuries vary dramatically in severity of the tissue damage and amount of contamination. At LANL, the majority of injuries were minor and the contamination amount less than the ALI.

Most of the wounds at LANL have been located on the hands or arms of the individual. A summary of the wounds and locations on the body that occurred at LANL during the period of 1960 - 1972 are listed in table 3 below (Johnson and Lawrence 1974). These wounds were primarily created using hand tools or sharp objects present during the machining of plutonium.

Table 3: Anatomical site of potentially contaminated wounds at LANL, 1960-1972 (Johnson and Lawrence 1974).

Body Location	Number of potentially contaminated wounds, 1960-1972
Fingers	96
Hands	18
Wrist-Arm	12
Head	10
Trunk	1
Not Recorded	26
Total	163

The maximum permissible body burden (MPBB) during the 1960 – 1972 time period was 40 nCi. Of the 163 potentially contaminated wounds, only 10 contained

estimated activities greater than 0.4 nCi (1% MPBB) (Johnson and Lawrence 1974). These are tabulated in table 4. When the activity exceeded an established level and if it was medically feasible, tissue was surgically excised to try and remove the contamination.

Table 4: Estimated activities in wounds with greater than 0.4 nCi and wound treatment (Johnson & Lawrence 1974).

Year	Activity Estimated (nCi)	Action Taken
1960	21	Surgically Excised
1960	10	Surgically Excised
1964	24	No Therapy
1966	6	No Therapy
1969	45	Surgically Excised
1969	10	No Therapy
1969	1.6	No Therapy
1970	20	Surgically Excised
1970	26	Surgically Excised
1971	16	Surgically Excised

In 2007 there have been two incidents at LANL that resulted in internal contamination through a wound. The first incident involved the use of screwdriver to pry a piece of plutonium metal off a fixed assembly. When the screwdriver slipped, it stabbed the worker in the opposite hand. This resulted in the deposition of approximately 20 nCi of plutonium in the tissue of the hand. During the second incident, a machinist was attempting to don a cotton glove in a gloved box when his arm slipped making forceful contact with the cutting tool puncturing his arm. Analysis of the cut showed approximately 1.3 nCi of plutonium contamination (Cantwell et al. 2007).

Treatment Options

When the activity of ^{239}Pu in the wound exceeds 37 Bq, it is recommended that the material in the wound be removed, though the final decisions on treatments are made by the attending physician in consultation with the health physics staff. The three primary methods used to remove the contaminated material from the wound are excision, flushing, and chelation therapy. These methods can be used individually or in combination. Excision is the physical removal of the surrounding tissue in an attempt to remove some of the material. Flushing the wound consists of spraying, suction, and wiping of the wound area in attempt to physically clean the wound of contamination. The last method, chelation therapy, is not used to remove the contamination from the wound site rather its purpose is to keep the material that has been absorbed by the blood from being deposited in various tissues. Chelation therapy is an intravenously administered chemical that will bind with the plutonium and not allow it to become deposited in various tissues throughout the body. This therapy allows the individual to excrete more of the material, but many studies have shown that this method must be done within a few hours after the intake to be effective (NCRP 1992).

Detector Systems Used to Assay Wounds

When an injury in the form of a cut, puncture, or laceration occurs and ^{239}Pu is injected underneath the skin, it is important to determine the location and activity of the contamination in the wound. Adequate sensitivity and accuracy of this measurement is critical to help guide decisions for medical intervention. The two primary detector systems, used to measure ^{239}Pu activity and location within a wound at LANL, are a thin crystal sodium iodide (NaI(Tl)) system and a high purity germanium (HPGe) system for contamination depth determinations. Both of these detector systems are used to measure the low-energy uranium L-x rays that are emitted. Each system is used to analyze wounds but the results from each are used to determine different aspects of the wound.

The general procedure for a potentially contaminated wound is to administer first aid for the victim, wash the wound thoroughly, and survey for surface contamination using an alpha detector. Bleeding is not always discouraged at first because this can

help flush contamination from the wound. Once the victim's wound is stabilized and cleaned to the best extent possible, the victim is transported to the Occupational Medicine facility, where the wound is measured for possible residual radioactivity. The activity in the wound is determined usually by a contact measurement using a NaI(Tl) system that is calibrated using a ^{239}Pu point source without tissue attenuation. If additional medical guidance for tissue excision is needed, the activity in the wound can be spatially mapped in the X,Y plane using the NaI(Tl) detector with collimated shielding and the Z plane (depth in tissue) using a HPGe detector system and analysis of the ratios of the 13 and 17-keV photopeaks in the energy spectrum.

The NaI(Tl) counting system is considered the workhorse at LANL for measuring the activity of ^{239}Pu in a wound because it is relatively easy to maintain and operate , inexpensive, has a high efficiency for low-energy photons, and the thin crystal results in low background response to higher-energy photons. Locating the wound is rather obvious but identifying the location of the contamination is not always as easy. Most wounds at LANL are mapped in the X and Y plane using a collimated sodium iodide system with a short count time (50 to 100 seconds) to help pinpoint the most radioactive locations in the wound. Mapping the wound is very useful for determining the locations for tissue excision while sparing surrounding tissue.

Measurement of wound activity uses two regions of interest (ROI). One region of interest contains the number of counts between 5 to 30 keV (the plutonium ROI); the second ROI contains the number of counts from 30 to 55 keV (the background ROI). The low-energy ROI records the x ray from plutonium plus background, while the higher-energy ROI contains the average background. Subtracting the high-energy ROI from the low-energy ROI gives the counts from the plutonium x rays only and is called the net counts. The activity in the wound can then be determined using the net counts and the known detector efficiency from calibration (Vasilik et al. 1978).

HPGe detectors used for wound counting also uses a thin active detector volume and thin entrance window. Both reduce the amount of Compton scattering in the spectrum allowing for higher detector sensitivity to low-energy interactions. Due to the

type of contact used in a p-type detector, x rays must travel through a dead layer of germanium crystal before interacting in the detector active volume. This attenuation greatly decreases the efficiency of the detector due to the high Z of the germanium dead layer (Knoll 1999). Detector efficiency of low-energy x rays is reduced due to the 11 keV K-shell binding energy of germanium. The decreased efficiency requires that longer count times be used, but HPGe systems have much better resolution this allows the user to distinguish the three low-energy uranium L-x ray emitted from the plutonium source. Three ROIs are used to determine the number of counts in each peak of interest that are associated with the characteristic x rays. By dividing the number of counts in a low-energy peak by that of a higher-energy peak it possible to estimate the amount of attenuation that has occurred in the tissue (Johnson and Lawrence 1974). Using the ratio and assuming a specific tissue type, the estimated depth of contamination can be calculated.

PROBLEM STATEMENT

Measurement of plutonium in wounds is difficult because the primary radiation of alpha particle emissions cannot be detected, if it is buried in the tissue. Resorting to the detection of the uranium L-shell x rays can also be difficult because they are emitted at very low-energies and abundances. This problem is only compounded by the small quantities that need to be measured (e.g., less than 37 Bq or 1 nCi).

Contact measurements are made to improve the sensitivity, but there is a significant dependence on counting efficiency based on the geometry of the source in the wound. The geometry includes the shape and orientation of the source (point, line, and angle of injection), the source to detector distance, and the amount of tissue between the wound and detector. Each of these can have a significant impact on the measurement of the ^{239}Pu in the wound, and thus, are important factors driving decisions related to medical intervention and the uncertainties (Hickman 1994). The magnitudes of these impacts have not been fully characterized for the LANL wound counting systems. The

goal of this study was to collect data characterizing the effects of source geometry, source to detector distance, and absorption in tissue, both individually and collectively.

CHAPTER II

METHODS AND MATERIALS

DETECTOR SYSTEMS

NaI(Tl) Detector System

The NaI(Tl) system that was used during the experiments consisted of a detector, high voltage (HV) power supply, spectroscopy amplifier, data acquisition computer card, and a desktop computer. The assembled components are shown in figure 2.

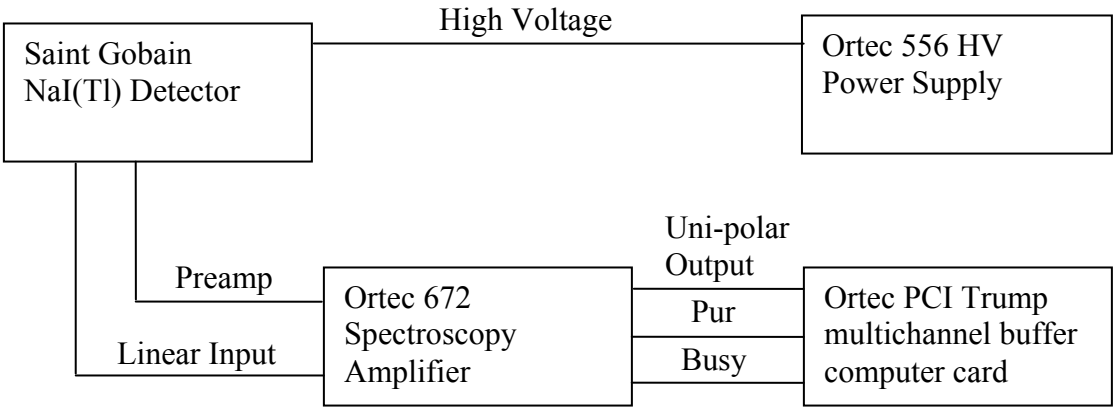

Figure 2: Diagram of NaI(Tl) system parts and assembly.

Saint-Gobain manufactured the detector as part of their Bicron "Monoline X-ray assembly" product line. The detector has a mu-metal case with a 25.4 mm diameter by 1 mm thick NaI(Tl) crystal mounted inside. A photomultiplier (PM) tube is optically coupled to the crystal and is also located inside the detector case. An aluminum entrance window is fixed in front of the crystal and is approximately 0.0254 mm thick. Saint-Gobain advertises this product to be able to measure x rays over the energy range from 10 to 200 keV with good efficiency.

The detector is powered using an Ortec 556 HV power supply NIM unit, which supplies a constant +700 V potential. An Ortec 672 spectroscopy amplifier NIM unit

contains the amplifier, preamplifier, pulse shape discriminator, and signal handling electronics. From the spectroscopy amplifier, the signal is sent to an Ortec PCI Trump multichannel buffer computer data acquisition card. This card is used to convert the analog signal from the amplifier to a digital signal that is used in the Ortec ScintiVision® Software. ScintiVision was developed specifically as a MCA emulation and analysis software for scintillation detector spectra. This software is used as the user interface to the detector for calibration, data collection, and spectrum analysis.

Energy Calibration

An energy calibration was done to ensure proper energy response and channel assignment over the photon energies used in the experiment. A 25.4 mm diameter ^{241}Am check source (27 ± 1.3 Bq) was used because it emits 13.9 and 59.54 keV photons with yields of 28% and 36.3%, respectively, and a low-yield photon at 26.36 keV (Ortec 2003). The source was placed 0.317 mm from the detector face and a photon energy spectrum was collected for fifteen hours. The relatively long count time ensured that the peaks in the spectrum would have a Gaussian shape. The ScintiVision software was used to mark the ROI of the two dominant peaks in the spectrum. A centroid channel of each peak was calculated using the software and assigned to their respective energies. The rest of the channels were assigned an energy based on the relational position of the two energy peaks and assuming a linear relationship between energy and channel.

Efficiency Calibration

A single-point efficiency calibration using a NIST traceable ^{239}Pu calibration source was performed. A NIST traceable source of 116 ± 6 Bq was counted for the duration of 24 hours to reduce error. One ROI was set covering the entire peak that was created by the 13.6, 17.2, 20.2-keV L-x rays. The ScintiVision software was used to calculate the net counts in the ROI and then divided by the live time to obtain a count rate (counts per second). The count rate was divided by the source activity and multiplied by 100 which resulted in an absolute efficiency of 2.74%. Although the

efficiency calibration was done, it was not used during the experiment due to the source geometry changing regularly, but only used for the MDA.

Minimum Detectable Activity

Minimum detectable activity (MDA) was calculated using the equations provided in the Ortec ScintiVision® users manual for no tissue attenuation (Ortec 2003). The calculation required that a background count be taken for all three of the count times of interest to determine the number of counts due to background in the ROI used for analysis. The gross counts in the ROI were used to calculate the minimum peak area (MPA), or the number of counts required for that ROI to be identified as a peak. Dividing the MPA by the product of the live time and detector efficiency of the ROI resulted in the MDA as tabulated in table 5.

Table 5: MPA and MDA for common count times used in the experiments ignoring tissue attenuation.

Live Time (sec)	MPA (counts)	MDA (nCi)
500	66.84	0.18
1000	89.51	0.12
1500	113.79	0.10

Experimental Setup

The detector was mounted in a fixed position for the duration of all measurements. As shown in figure 3, the detector was clamped into position and not easily adjustable. Below the detector was a platform used to hold the source and tissue substitute to simulate a wound count. This platform was adjustable to allow for the wound phantom to be modified as needed.

Figure 3: Image of the NaI(Tl) wound counting system.

Analysis

The poor resolution of the NaI(Tl) detector system caused all three of the low-energy x ray peaks to appear as a single peak in spectrum. Therefore, a single ROI was used to determine the number of counts generated by all three low-energy x rays. The ScintiVision® software was used to calculate the net counts plus or minus one standard deviation. Net counts were used to calculate the absolute efficiency. The absolute detection efficiency and the uncertainty were calculated as shown in equations 1 and 2, respectively. This was done for all NaI(Tl) measurements to assess the efficiency response as a function of source shape, geometry, and tissue attenuation.

$$\varepsilon_{abs} = \left[\frac{\left(\frac{NC_{ROI}}{LT} \right)}{A_D \left(\frac{C_X}{C_D} \right)} \right] \qquad (1)$$

$$\sigma_{\varepsilon_{abs}} = \sqrt{\left[\frac{\left(\frac{1}{LT}\right)}{A_D\left(\frac{C_X}{C_D}\right)}\right]^2\left(\sigma_{NC_{ROI}}\right)^2 + \left[\frac{\left(\frac{NC_{ROI}}{LT}\right)}{\left(A_D\right)^2\left(\frac{C_X}{C_D}\right)}\right]^2\left(\sigma_{A_D}\right)^2 + \left[\frac{\left(\frac{NC_{ROI}}{LT}\right)}{A_D\left(C_X\right)}\right]^2\left(\sigma_{C_D}\right)^2 + \left[\frac{\left(\frac{NC_{ROI}}{LT}\right)}{A_D\left(\frac{\left(C_X\right)^2}{C_D}\right)}\right]^2\left(\sigma_{C_X}\right)^2} \quad (2)$$

where

ε_{abs} = absolute efficiency;

NC_{ROI} = net counts for the ROI;

LT = live time;

A_D = activity of the disk source;

C_X = count rate of the masked source measured on the Berthold alpha counter;

C_D = count rate of the unmasked disk source measured on the Berthold alpha counter;

$\sigma_{NC_{ROI}}$ = error in the net counts of the ROI;

σ_{A_D} = error in the activity of the disk source;

σ_{C_D} = error in the Berthold counts of the disk source; and

σ_{C_X} = error in the Berthold counts of the masked source;

HPGe Detector System

The primary function of the HPGe detector was to determine the depth of the contamination in a wound by analyzing the relative attenuation of two of the low-energy x rays emitted by the plutonium contamination. The HPGe detection system consisted of a detector preamplifier assembly, high voltage (HV) power supply, amplifier, multichannel buffer (MCB), data acquisition computer card and desktop computer. Figure 4 shows the detector assembly arrangement.

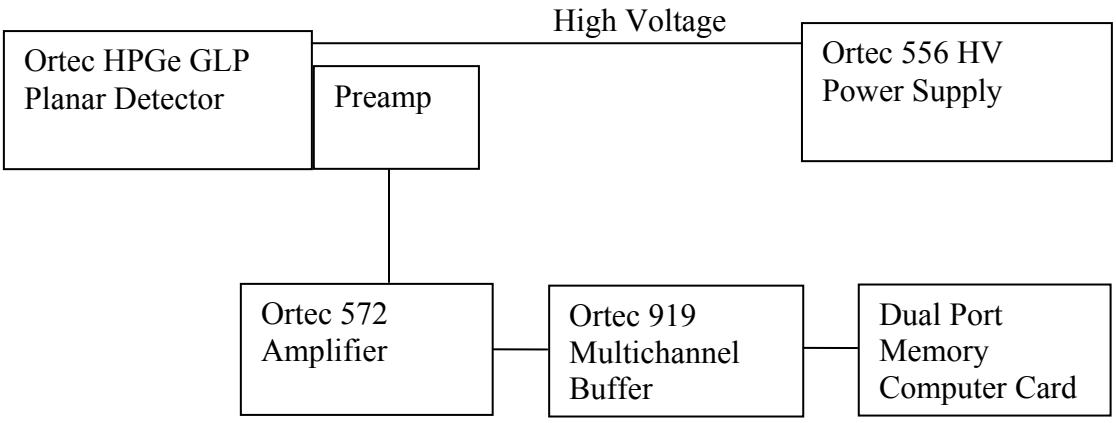

Figure 4: Diagram of HPGe system parts and assembly.

The detector was manufactured by Ortec and was a GLP series high-purity, germanium, p-type detector. The detector was a low-energy photon spectrometer in the planar configuration with a 0.3 μm thick ion-implanted front contact. To reduce attenuation of low-energy photons, a thin beryllium entrance window, 0.254 thick, was used to seal the front of the cryostat. The detector active crystal was 13 mm thick with a diameter of 36 mm. This detector was advertised to be useful over the approximate energy range from 3 keV to 300 keV.

An Ortec 556 HV power supply is used to supply a constant bias voltage of negative 800 volts to activate the crystal. A signal preamplifier (located inside the detector housing) sends a signal to the Ortec 572 amplifier. The analog signal leaves the amplifier and is routed to the Ortec 919 MCB, which was an analog to digital converter and a multichannel analyzer. Lastly, the signal was sent to a data acquisition computer card and analyzed using the Ortec GammaVision® gamma spectroscopy software (Ortec 2006).

Energy Calibration

Energy calibration was done utilizing a 4,398 ± 44 Bq Am-241 source with a diameter of 25.4 mm. During the calibration, the source was placed directly in front of the detector, touching the entrance window. The high resolution of the detector allowed for a three point calibration using the 13.9 keV, 26.36 keV, and 59.54 keV gamma-ray peaks. A linear relationship was established between channel number and energy from the three data points. This relationship was used by the GammaVision® software to assign energies to the rest of the channels in the spectrum.

Efficiency Calibration

The efficiency calibration used the same check source. A twenty-four hour count was made to ensure good Gaussian shape of the peaks and to reduce counting errors due to low-count rates. The GammaVision® software was used to create a source certificate of the ^{239}Pu check source. This was used with the software to create a calibration file. A polynomial fit was used for the efficiency versus energy calibration with relative errors less one percent. The measured efficiency was used in the calculation of the MDA.

Minimum Detectable Activity

Minimum detectable activity (MDA) was calculated using the equations provided in the Ortec GammaVision® users Manual ignoring tissue attenuation (Ortec 2006). MDA calculations used a 1000 second count time because that was the count time used during all data collection. Separate MDAs were calculated for the two low-energy peak ROIs of interest (i.e. 13 keV and 17 keV). The calculations required that a background count be taken for 1000 seconds to determine the number of counts due to background in each ROI. The gross background counts in each ROI were used to calculate the minimum peak areas, or the number of counts required in that ROI to be statistically identified as a peak. Dividing the MPA by the product of the live time and detector efficiency of the ROI resulted in the MDA as tabulated in table 6.

Table 6: HPGe minimum detectable activities ignoring tissue attenuation.

Peak Energy	Live Time	MPA	MDA
(keV)	(sec)	(counts)	nCi
13.5	1000	57.74	0.36
17.4	1000	59.88	0.35

Experimental Setup

The detector was placed on a cart that was adjustable vertically to allow for the detector head to be placed in front of test assemblies. Figure 5 shows the HPGE detector and source platform. A shelf was attached to the wall and held the source and tissue substitute during the experiments. The source and tissue substitute were moved around in front of the detector face while the detector was held stationary to reduce the possibility of detector damage.

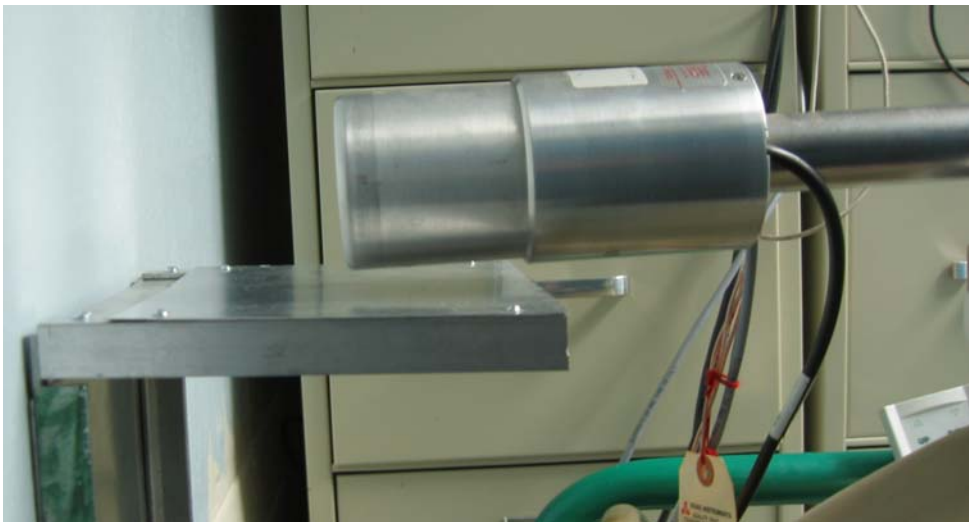

Figure 5: HPGE detector counting system.

Analysis

The HPGe detector system has the advantage of good resolution, which allows for the low-energy x ray peaks to be resolved individually in the spectrum. Using the GammaVision® software, an ROI was set for each peak to determine the net counts within each region. Lower-energy photons should be attenuated more than higher-

energy photons in materials such as tissue. Theoretically, the ratio of the number of counts in the lower-energy peak divided by counts in the higher-energy peak would decrease with increased tissue thickness. Equations 3 and 4 below were used to determine the measured ratio from the two low-energy peaks, determine the relationship between the ratio and depth in a tissue substitute, and assess the associated uncertainties:

$$R_{(13/17)} = \left(\frac{NC_{13}}{NC_{17}} \right), \tag{3}$$

$$\sigma_{R_{(13/17)}} = \sqrt{\left(\frac{1}{NC_{17}} \right)^2 * \left(\sigma_{NC_{13}} \right)^2 + \left(\frac{NC_{13}}{\left(NC_{17} \right)^2} \right)^2 * \left(\sigma_{NC_{17}} \right)^2}, \tag{4}$$

where

$R_{(13/17)}$ = peak to peak ratio;

NC_{13} = net counts from the 13.5 keV peak ROI;

NC_{17} = net counts from the 17.4 keV peak ROI;

$\sigma_{R_{(13/17)}}$ = peak to peak ratio error;

$\sigma_{NC_{13}}$ = error in net counts of 13.5 keV peak ROI; and

$\sigma_{NC_{17}}$ = error in net counts of 17.4 keV peak ROI.;

EFFECTS OF TISSUE ATTENUATION

Measurement of the low-energy x rays from plutonium decay depends on the detector geometry and efficiency. The measurement becomes more complicated if that the plutonium is buried in tissue. Therefore, measurements made in wound monitoring have to account for photon attenuation in tissue. Experiments with tissue substitutes were conducted to characterize the LANL wound counting systems with respect to tissue attenuation.

Tissue Substitute Selection

The selection of a representative tissue substitute material was far from trivial, but much guidance can be gained from the ICRU Report 44. It was determined that most wounds occurred in the hand or arm area of the body and in tissue best described as soft or adipose tissue. It was important that the material chosen as a tissue substitute had approximately the same absorption and scatter characteristics as that of the actual tissue over the appropriate range of photon energies (ICRU 1989).

^{239}Pu emits uranium L x rays with the lowest energy of about 13 keV, while ^{241}Am, which is often part of the plutonium mixture found in wounds, emits gamma rays with energies of 59.5 keV. Therefore, energy range for important gamma-rays and x rays associated with wound counts was from 10 to 100 keV. This means the substitute material needs to simulate adipose tissue with respect to gamma-ray attenuation for energies up to 100 keV. It was also determined that the material should be a solid at room temperature and not require excessive amounts post processing such as machining or molding.

Photons can interact in tissue through photoelectric absorption, Compton scattering, pair production, and photonuclear absorption (ICRU 1989). At the energies of interest, 10 to 100 keV, the dominant interaction will be photoelectric absorption. The remainder of the interaction cross section will be from Compton (incoherent) and coherent scattering. Since the energies of interest are so low, the Compton interaction cross section is low and there would be little photon buildup or scatter into the detectors. Therefore, the experimental geometry can best be described as narrow beam, which makes the mass attenuation coefficient the most important parameter to compare between adipose tissue and the simulant (Attix 2004).

ICRU-44 includes tables of mass attenuation coefficients for materials that have been commonly used as tissue substitutes. From these tables, three materials were chosen as candidates for tissue substitutes. The selected materials were acrylic, A-150 plastic, and nylon 6, which are all easily obtained polymer plastics capable of being molded or machined. Figure 6 shows the percent difference of the mass attenuation

coefficient of each material with respect to adipose tissue over the range of energies of significance. For this experiment, the energies between 10 and 30 keV were most important. In this energy range, acrylic, A-150, and nylon produced maximum mass attenuation percent differences of 3, 27, and 13 percent, respectively.

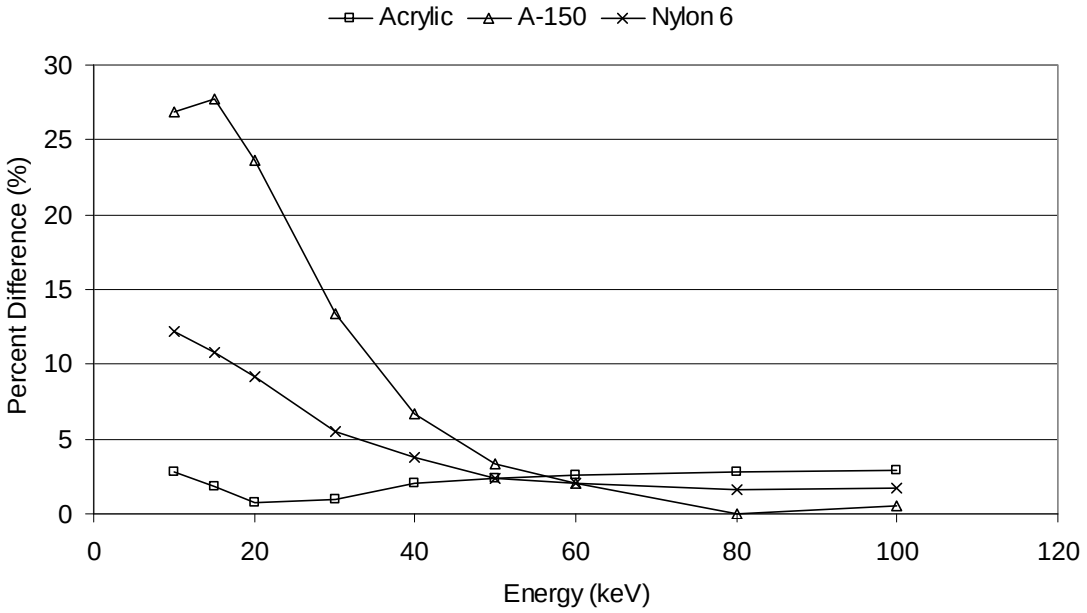

Figure 6: Mass attenuation coefficient percent difference of each material with respect to adipose tissue (ICRU 1989).

This analysis showed that acrylic had the most similar mass attenuation properties to adipose tissue over the energy range of interest. A cost analysis further confirmed that acrylic would be a good option for use in the experiment because it was the least expensive of the three materials and it was the easiest to get from a variety of suppliers. Therefore, based on the physical characteristics, mass attenuation properties, cost, and availability, acrylic was chosen as the tissue substitute for all experiments.

EXPERIMENTAL PROTOCOLS

Source Shape

Source shape plays an important role in the characterization of the LANL detection systems. The LANL wound counters are calibrated using a 25.4 mm diameter disk source. The activity on this disk source is not homogeneously distributed across the disk though most of the activity was found to be in the center portion of the disk. However, the geometry of contamination in actual wounds can vary dramatically from that of the calibration source with two likely geometries being a small point or line source of varying angles in the tissue. The shape and size of the source will likely have an effect on the detector efficiency due to the solid angle created by each source.

To better understand the effect of a few common source shapes and wound geometries, experiments were conducted using disk, line, and point sources. The line and point sources were created by masking the disk source using at 0.45 mm thick sheet of stainless steel, which was machined to create a specific shape. This mask, when used as a shield the over a ^{239}disk source, provided a 98.1% reduction in photon emission. The mask for the point source had a hole with a diameter of 0.411 mm covering all but the center of the disk source. The mask opening for the line source was 2 mm wide with a length of 21.8 mm and passed through the center of the disk source. To determine the activity of the masked sources, an EG&G Berthold gas proportional counter was used to measure the gross alpha counts from each source. The ratio created by dividing the masked source count rate by that of the uncovered disk source was the fraction of the original activity present in the disk source. Therefore, the product of the ratio and the certified activity of the disk source was the activity for each of the masked sources.

Source Distance and Angular Effects

The distance between the source and the detector was an important parameter to control due to its effect on efficiency. When the source is moved further away from the detector the solid angle seen by the detector becomes smaller and reduces the amount of

radiation reaching the detector, which decreases detector efficiency. To characterize this effect for each system, the detector was fixed and the point and line sources were moved progressively further away, as illustrated in figure 7. The solid angle of the line source can also be affected by changing the angle with which it is oriented to the detector. Measurements with the line source were conducted using angles of 0°, 45° and 90° relative to the detector face. Figure 8 illustrates the experiment used to investigate angular effects of the line source.

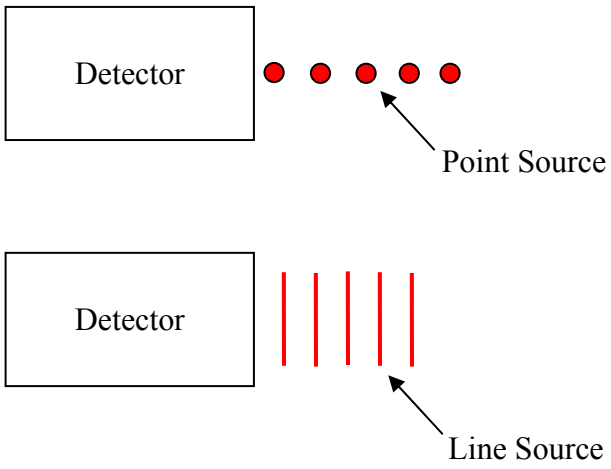

Figure 7: Experimental setup for characterizing geometry effects of distance for a point (top) and line source (bottom).

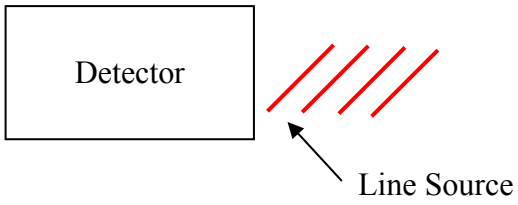

Figure 8: Experimental setup for examining geometry effects by angular displacement.

Attenuation Effects

Attenuation of the x rays in tissue is another factor that contributes to the reduction in absolute detector efficiency. To characterize the effects of attenuation, each source (point, line, disk) was held a fixed distance from the detector and counted while the thickness of tissue substitute between them was increased as shown in figure 9. The thickness of tissue substitute was increased until it was equal to the distance between the source and the detector.

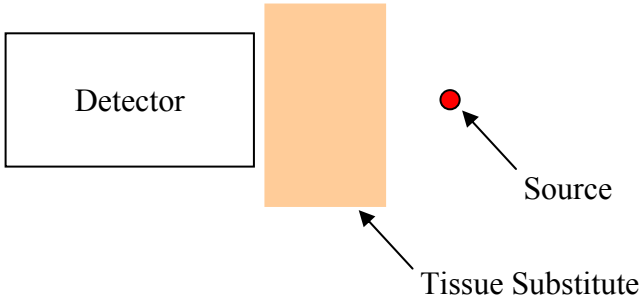

Figure 9: Experimental setup to characterize the effect of attenuation.

Combined Attenuation and Geometry Effects

In reality, measuring wound contamination must account for the combined effects of geometry and attenuation at the same time, not independently. Therefore, it was important to create a set of experiments to characterize the combined effects. Figure 10 illustrates the setup used to investigate the effects of source distance combined with attenuation of the x rays. While figure 11 illustrates the effects of line source angular displacement combined with attenuation.

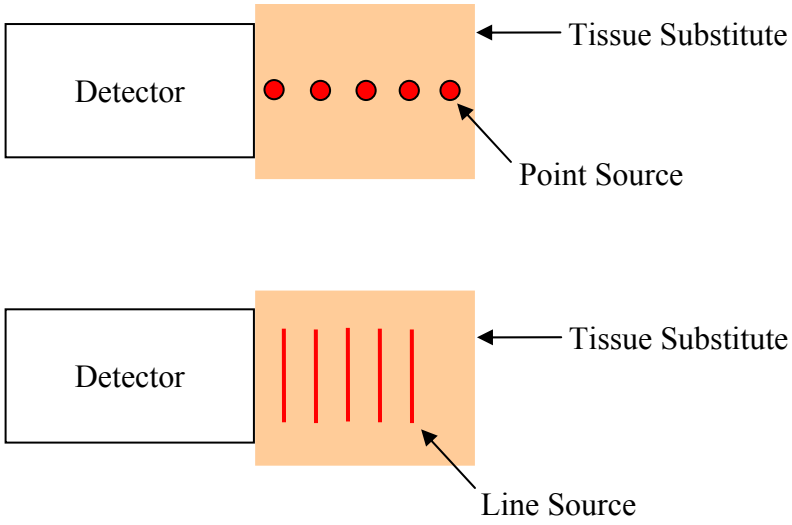

Figure 10: Experimental setup for characterizing geometry effects of distance and attenuation due to tissue for a point source (top) and line source (bottom).

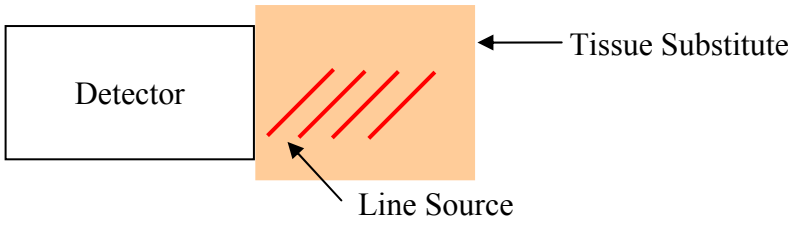

Figure 11: Experimental setup for examining geometry effects of angular displacement and attenuation due to tissue for a line source.

MONTE CARLO TECHNIQUES

Monte Carlo techniques can be extremely helpful for predicting transport of photons, neutrons, and higher-energy electrons through materials. Monte Carlo computer codes allow the user to save resources by creating a model of the system of interest and transporting particles based on the physics of the interactions between particles and materials. This can be highly efficient because Monte Carlo transport models can be used to evaluate many different experimental variations without the cost

(financial and time) of the many actual measurements that might be needed. In this study, for example, it was realistic to expect the contamination in a puncture wound to be distributed along the path of the wound, but the number of possible angles is infinite. Therefore, the Monte Carlo code MCNP5 was used to examine the effects of varying the angle of a line source in tissue on detection efficiency and peak-to-peak ratio.

Monte Carlo modeling also helped with the analysis of the effects of a "true" line source on counting efficiency for the x rays studied. First, the masked source used in the experimental measurements was not a perfectly "true" line source because the activity was not perfectly distributed across the disk face; the concentration was higher towards the center of the disk. Secondly, experimental measurements made at 45° and 90° also did not represent a "true" line source because the backing plate of the source shielded many of the x rays from the detector. The Monte Carlo model allowed an analysis of a true line source without the effects of the source plate.

NaI(Tl) Detector Model

Using the technical design documents provided by Saint Gobain, the NaI(Tl) detector was modeled in MCNP5 as shown in figure 12. Modeling of the NaI(Tl) crystal was done ignoring the thallium dopant because it makes up a small percent of the mass and the actual composition is a trade secret. The elemental tissue composition was modeled as adipose tissue from the ICRU-44 report. A single pulse height tally was applied to the NaI crystal to create simulated detector response. Fifty million photons were transported using the emission spectrum of ^{239}Pu's twenty two x rays with energies that ranged from 9 to 150 keV (Exploring the Table of Isotopes Berkeley Labs). All MCNP input decks for the NaI(Tl) are listed in Appendix A.

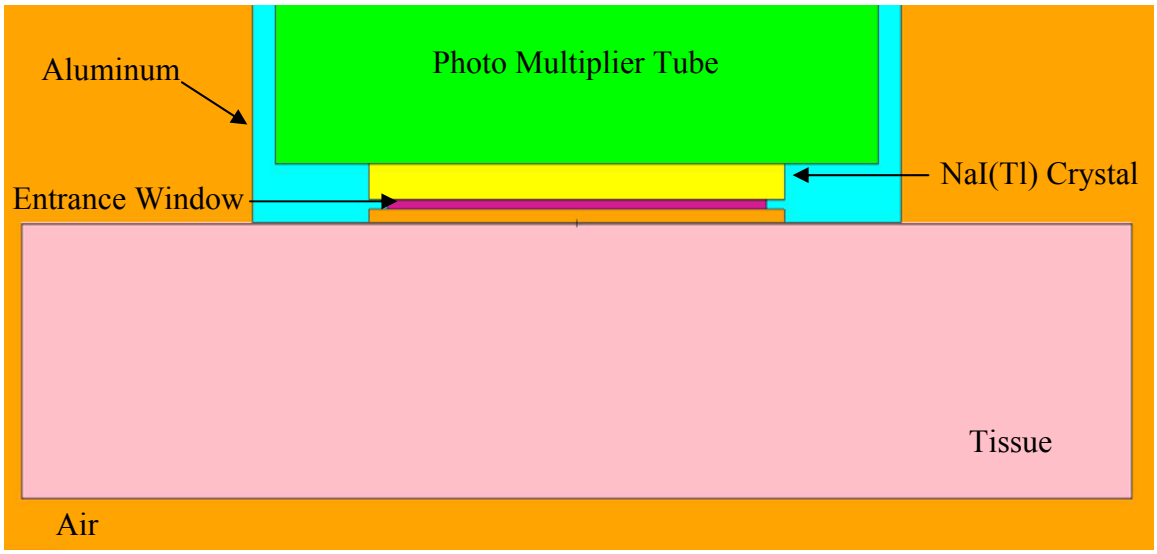

Figure 12: NaI(Tl) Detector MCNP Model.

Analysis

The NaI(Tl) model output data was analyzed using methods similar to those of the actual system using equation 5. An MCNP f8 tally was used to sum the number of particles that interacted in the NaI(Tl) crystal and sort them in bins according to their energy deposition. Using an ROI that covered the entire range from 3.8 keV to 30 keV, similar to the actual detector, all counts generated by the three energies of interest were summed together. Since only the x rays from plutonium decay were generated in the model, the number of particles tracked is only a fraction of the total number of disintegrations that would actually occur. Therefore, the number of particles tracked was divided by the sum of the yields for the energies in the model to obtain the total number of x rays that should have been emitted, and determine the absolute efficiency as shown in equation 5:

$$\varepsilon_{abs} = \left[\frac{C_{ROI}}{\left(\frac{NP}{\sum Y(i)} \right)} \right] \qquad (5)$$

where

ε_{abs} = absolute efficiency;

C_{ROI} = total counts in the ROI for all three energies together;

NP = number of particles tracked through the model; and

$\sum Y(i)$ = sum of the actual yields from all energies ran through the model;

HPGe Detector Model

The HPGe detector was modeled using information from the Ortec owner's manual, which described the detector head in enough detail to create the model shown in figure 13. Pure germanium was used to model the crystal which included a thin dead layer on the front of the crystal face. Once again, the elemental tissue composition was modeled as adipose tissue from the ICRU-44 report. A pulse height tally was applied to the active portion of the germanium crystal to mimic the detector response. The same source and tissue geometries used in the NaI(Tl) model were also used in the HPGe model. All MCNP input decks for the HPGe detector are listed in Appendix A.

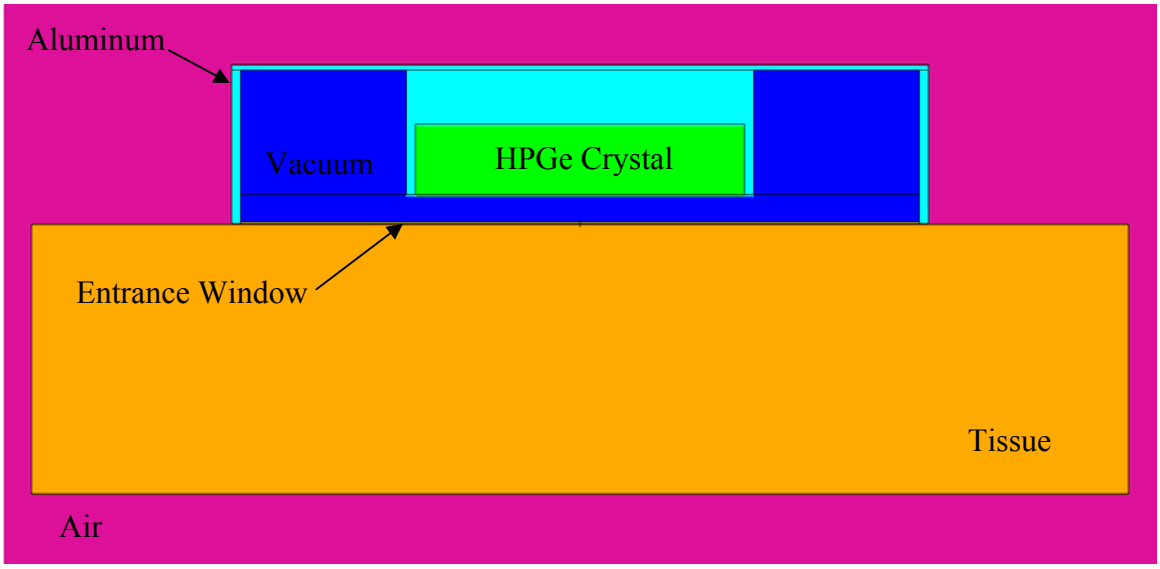

Figure 13: HPGe Detector MCNP Model.

Analysis

MCNP calculations produced output files that contained information about the number of particles interacting in the HPGe crystal. These were sorted into bins according to energy deposition. Because the HPGe detector has the ability to resolve the peaks of interest individually, an ROI for each peak was established. The counts in the ROIs were divided by one another, as shown in equation 6, to generate a peak-to-peak ratio similar to the actual detector analysis:

$$R_{(13/17)} = \left(\frac{C_{13}}{C_{17}} \right) \tag{6}$$

where

$R_{(13/17)}$ = peak to peak ratio;

C_{13} = total counts from the 13.5 peak ROI; and

C_{17} = total counts from the 17.4 peak ROI;

CHAPTER III

RESULTS

SODIUM IODIDE RESULTS

Distance Effects

When the source was moved away from the detector, the number of counts recorded was expected to decrease. This decrease will mostly be due to the change in geometry, with little impact of air attenuation occurring within the maximum 20 mm source to detector distance (1-3 % air attenuation). Figure 14 shows the relationship between efficiency and increasing distance for all five source-shape configurations. The calculated mean absolute efficiency and standard deviations are tabulated in table 7. Line source distance from the detector is the distance of the closest point of the line source to the detector. The disk, point, and line 0° sources were affected the most due to the increased distance. The line sources oriented at the 45° and 90° angles to the detector resulted in the lowest efficiencies at all distances and the smallest change in efficiency due to the increased distance. Decrease in efficiency over the range of the distance was about a factor of five for the disk and point source but was only about a factor of three for the angled line sources.

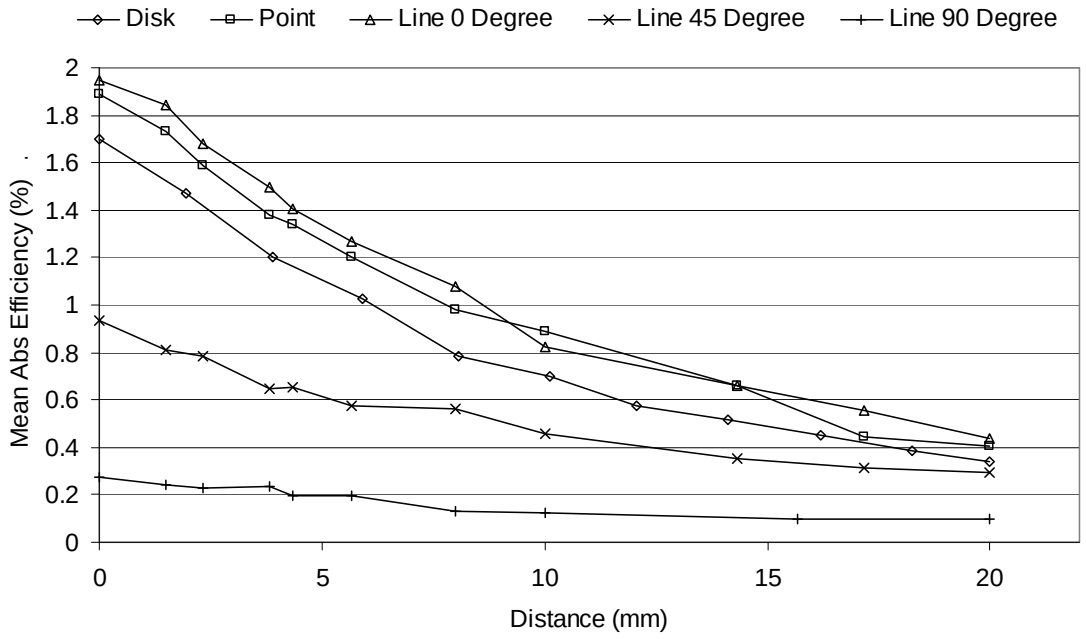

Figure 14: Efficiency response for the source distance from detector.

Table 7: Efficiency response with error due to source distance from detector for all source geometries.

Source	Disk		Point		Line 0° Angle		Line 45° Angle		Line 90° Angle	
Distance	Efficiency	Error	Efficiency	Error	Efficiency	Error	Efficiency	Error	Efficiency	Error
(mm)	(%)	STD	(%)	STD	(%)	STD	(%)	STD	(%)	STD
0	1.70	0.09	1.89	0.10	1.95	0.11	0.94	0.06	0.27	0.02
1.49	1.47	0.08	1.73	0.09	1.84	0.10	0.81	0.05	0.24	0.02
2.34			1.59	0.09	1.68	0.09	0.79	0.05	0.23	0.02
3.83	1.20	0.07	1.38	0.08	1.50	0.09	0.65	0.04	0.24	0.02
4.33	1.03	0.06	1.34	0.07	1.40	0.08	0.65	0.04	0.19	0.02
5.67			1.21	0.07	1.27	0.07	0.58	0.04	0.19	0.02
8.01	0.78	0.04	0.98	0.06	1.08	0.06	0.56	0.04	0.13	0.02
10	0.70	0.04	0.89	0.05	0.83	0.05	0.46	0.04	0.13	0.01
14.33	0.52	0.03	0.66	0.04	0.66	0.04	0.36	0.02	0.10	0.01
17.16	0.42	0.03	0.44	0.03	0.55	0.04	0.31	0.02		
20	0.34	0.02	0.40	0.03	0.43	0.03	0.29	0.02	0.09	0.01

Attenuation Effects

For this set of measurements, each source was fixed, 20 mm from the detector while an increasing amount of tissue substitute was placed between the source and detector. The line source distance from the detector was the distance from the closest point of the line source to the detector. The absolute detector efficiency decreased due the increased amount of attenuation that occurred in the tissue substitute, as illustrated in figure 15. Detector efficiency of the point and line 0° source decreased at approximately the same rate, and both were higher than that for the disk source for all absorber thicknesses. The efficiency of both the 45° and 90° line sources was low and changed less relative to all other source geometries. The calculated values of mean and standard deviations of the absolute detector efficiency are tabulated in table 8.

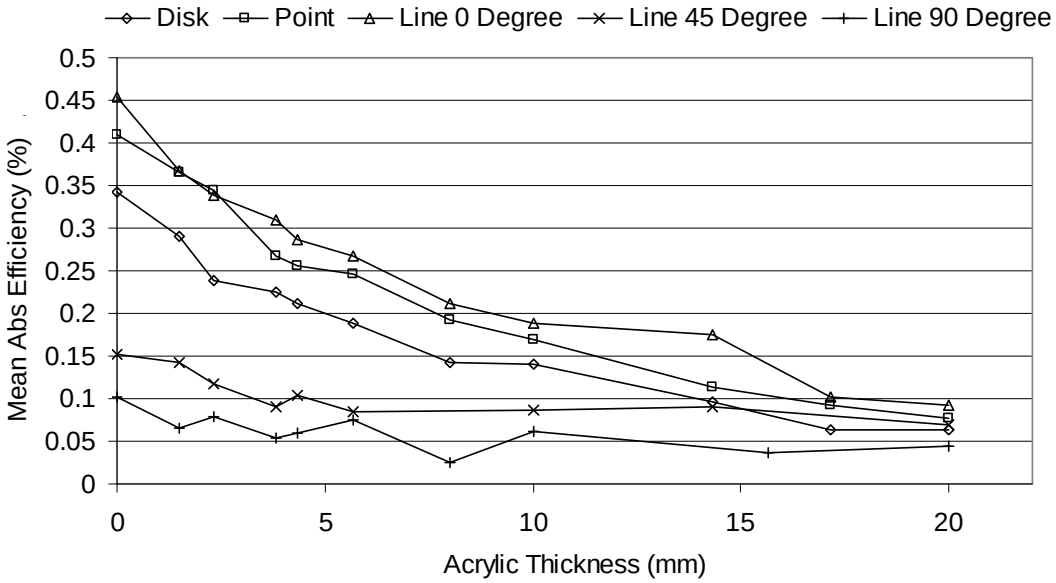

Figure 15: Efficiency response due to tissue substitute attenuation for all source geometry types.

Table 8: Efficiency Response with error due to attenuation.

Acrylic	Disk		Point		Line 0° Angle		Line 45° Angle		Line 90° Angle	
Thickness	Efficiency	Error	Efficiency	Error	Efficiency	Error	Efficiency	Error	Efficiency	Error
(mm)	(%)	STD	(%)	STD	(%)	STD	(%)	STD	(%)	STD
0	0.34	0.02	0.41	0.03	0.45	0.03	0.15	0.02	0.10	0.02
1.49	0.29	0.02	0.37	0.02	0.37	0.03	0.14	0.01	0.07	0.02
2.34	0.24	0.02	0.34	0.02	0.34	0.02	0.12	0.02	0.08	0.02
3.83	0.23	0.02	0.27	0.02	0.31	0.02	0.09	0.01	0.05	0.02
4.33	0.21	0.01	0.26	0.02	0.29	0.02	0.10	0.01	0.06	0.02
5.67	0.19	0.01	0.25	0.02	0.27	0.02	0.08	0.01	0.08	0.02
8.01	0.14	0.01	0.19	0.02	0.21	0.02	0.09	0.01	0.02	0.02
10	0.14	0.01	0.17	0.01	0.19	0.01	0.09	0.01	0.06	0.02
14.33	0.10	0.01	0.11	0.01	0.17	0.01				
17.16	0.06	0.01	0.09	0.01	0.10	0.01				
20	0.06	0.01	0.08	0.01	0.09	0.01	0.07	0.01	0.04	0.02

Combined Effects

Figure 16 illustrates the absolute efficiencies of the detector when the source was moved away from the detector and the gap between them filled with tissue substitute. Line source distance from the detector is the distance of the closest point of the line source to the detector. The detector response to the combined effects of attenuation and distance was similar to what was expected. Efficiency responses of the detector to the disk, point, and line 0° sources were very similar, initially decreaseing rapidly. Likewise, the responses created by the line sources placed at an angle to the detector were small over the entire range. The calculated values of mean and standard deviations of absolute detector efficiency are tabulated in table 9.

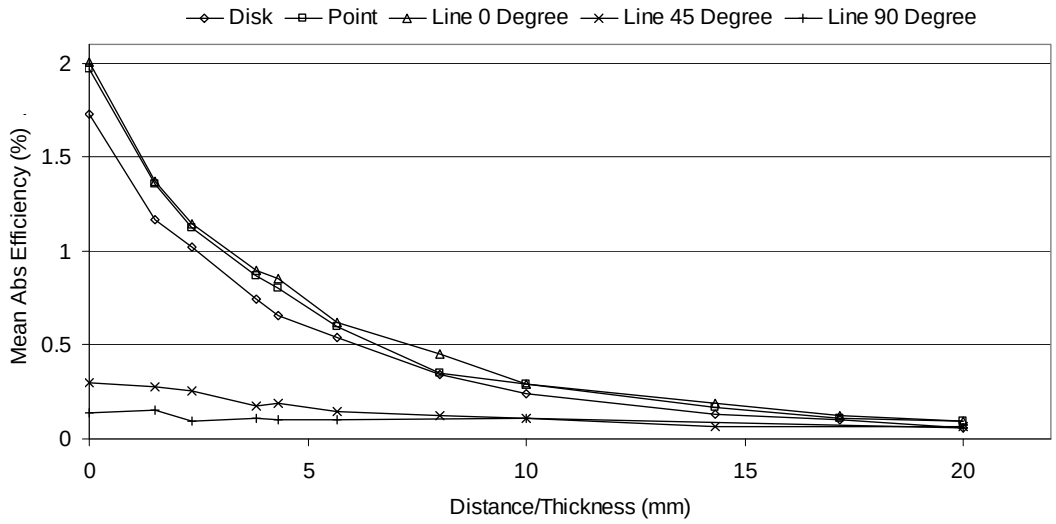

Figure 16: Efficiency response due to combined effects.

Table 9: Efficiency Response with error due to combined effects.

Acrylic	Disk		Point		Line 0° Angle		Line 45° Angle		Line 90° Angle	
Thickness	Efficiency	Error	Efficiency	Error	Efficiency	Error	Efficiency	Error	Efficiency	Error
(mm)	(%)	STD	(%)	STD	(%)	STD	(%)	STD	(%)	STD
0	1.72	0.09	1.97	0.11	2.00	0.11	0.30	0.02	0.14	0.02
1.49	1.17	0.06	1.36	0.08	1.37	0.08	0.28	0.02	0.15	0.02
2.34	1.02	0.05	1.13	0.07	1.15	0.07	0.26	0.02	0.09	0.01
3.83	0.75	0.04	0.87	0.05	0.90	0.06	0.18	0.02	0.11	0.02
4.33	0.66	0.04	0.80	0.05	0.85	0.05	0.19	0.02	0.10	0.01
5.67	0.54	0.03	0.60	0.04	0.62	0.04	0.15	0.02	0.10	0.01
8.01	0.34	0.02	0.35	0.03	0.45	0.03	0.12	0.02		
10	0.24	0.02	0.29	0.02	0.29	0.04	0.11	0.01	0.11	0.01
14.33	0.13	0.01	0.17	0.02	0.19	0.04	0.06	0.01		
17.16	0.10	0.01	0.11	0.02	0.12	0.04				
20	0.06	0.01	0.09	0.02	0.09	0.04	0.06	0.01	0.06	0.01

Comparison of Reduction in Counting Efficiency

The previous results show that counting efficiency decreases with both the distance and thickness of absorber between the source and the detector. This reduction in counting efficiency was particularly pronounced for the disk, point and 0° line source. Figure 17 shows the relative reduced efficiency (ratio of absolute efficiency of source contacting the detector surface to the absolute efficiency of the source at some distance and absorber thickness) as a function of the distance and absorber thickness for all source geometries. The results show that efficiency drops most rapidly and approximately equally, for the disk, point, and 0° line sources. Therefore, it would be particularly important to determine and apply depth correction factors for each of these source geometries to accurately determine the amount of plutonium in a wound.

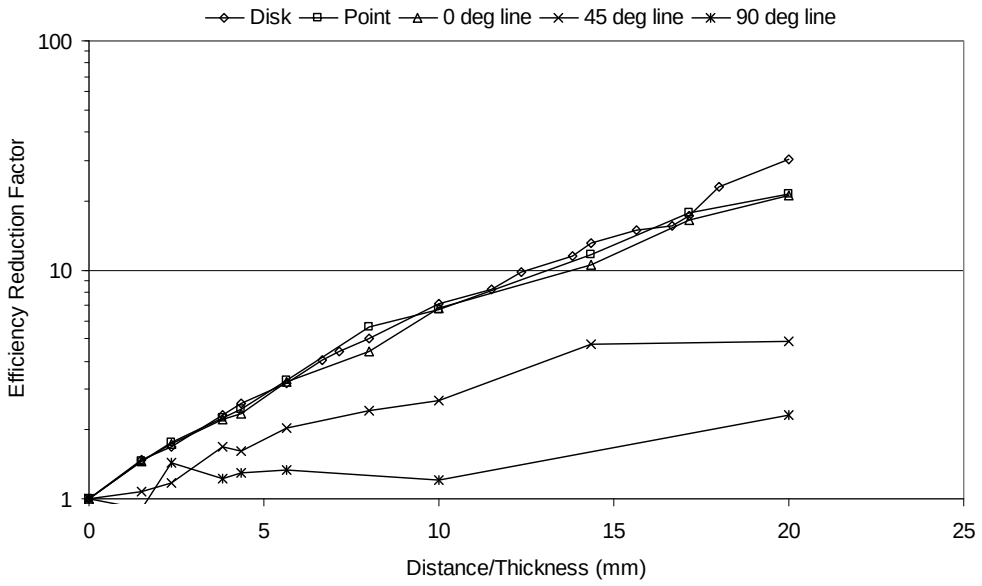

Figure 17: Reduction in efficiency due to combined effects of distance and thickness of absorber for all source geometry types.

HIGH PURITY GERMANIUM RESULTS

Distance Effects

Figure 18 illustrates the detector 13 keV to17 keV peak-to-peak ratios as the source is moved further away form the detector. The peak ratio for the point source is fairly unchanged through the entire distance and oscillates around a value of about 1.0. This was expected because the x ray energies would not be attenuated significantly in air between the source and the detector. The ratio for the line source at an angle of 0° is also rather unchanged until about 10 mm. Then it becomes more sporadic like that of the line 45° source. The large fluctuations are likely due to the low count rates, which contribute to the variability of the ratio, and are especially pronounced at the greater distances. Additionally, because of lower counting efficiency, the 90° line source only produced three statistically significant data points that were above two standard deviations of net background counts. These data suggest the importance of having high activities and long count times for accurate depth of burial determinations, especially for unfavorable counting geometries with small solid angles. Calculated peak-to-peak ratios have been tabulated with one standard deviation in table 10.

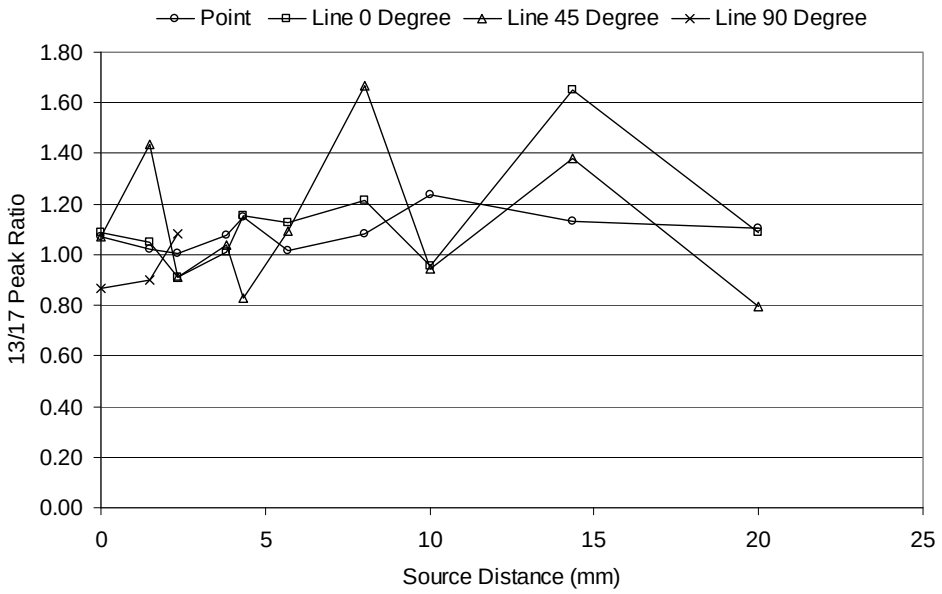

Figure 18: Peak ratios as a function of distance from the detector.

Table 10: Results of 13 keV to 17 keV peak ratios with one standard deviation (STD) for distance effects only.

Distance	Point Source		Line 0° Angle		Line 45° Angle		Line 90° Angle	
mm	Ratio	STD	Ratio	STD	Ratio	STD	Ratio	STD
0	1.07	0.11	1.09	0.13	1.07	0.25	0.87	0.32
1.49	1.02	0.09	1.05	0.12	1.44	0.39	0.90	0.35
2.34	1.01	0.11	0.91	0.10	0.91	0.18	1.08	0.41
3.83	1.08	0.11	1.01	0.13	1.04	0.23	0.82	0.71
4.33	1.15	0.13	1.15	0.17	0.83	0.17	26.00	450.88
5.67	1.01	0.11	1.12	0.17	1.10	0.31	1.42	3.57
8.01	1.08	0.14	1.21	0.22	1.67	0.44	0.40	0.45
10	1.24	0.18	0.96	0.17	0.94	0.18		
14.33	1.13	0.19	1.65	0.26	1.38	0.41		
20	1.10	0.24	1.09	0.21	0.80	0.33		

Attenuation Only

The source was fixed 10 mm from the detector face while increasing amounts of tissue substitute were placed between the detector and the source. Data collected using the line sources held at positive angles with respect to the detector face were not used because total net counts were less than two standard deviations of background error. For the point and 0° line source, the 13 keV to 17keV peak-to-peak ratios showed a decreasing trend for increasing amounts of tissue attenuation as shown in figure 19. Calculated peak-to-peak ratios have been tabulated with one standard deviation in table 11.

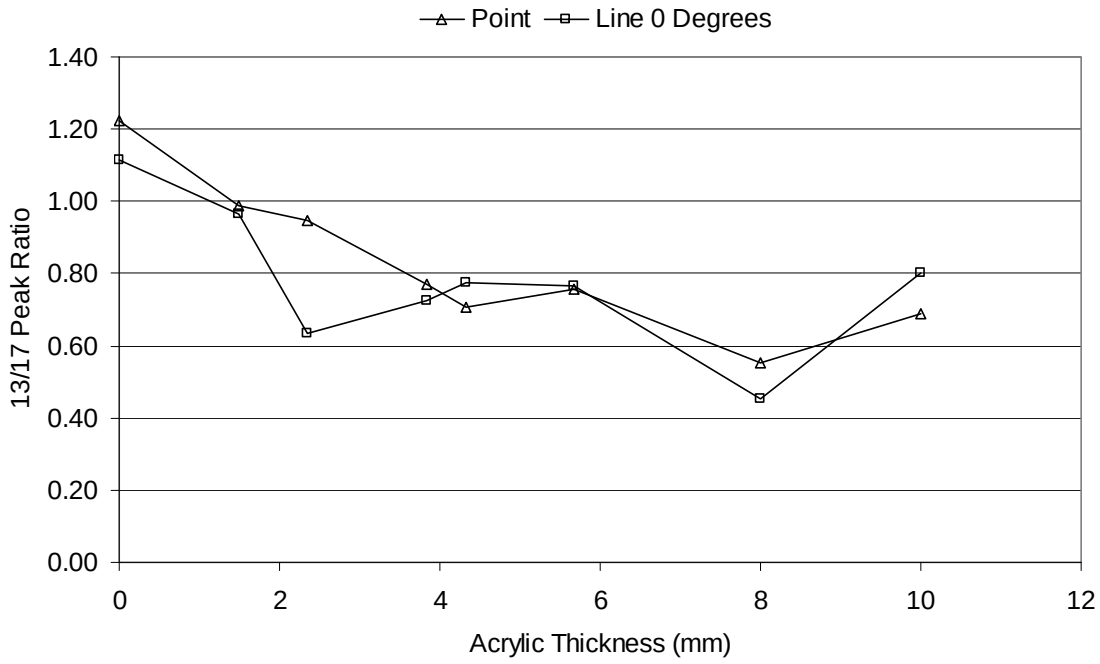

Figure 19: Peak ratio change due to attenuation.

Table 11: Results of 13 keV to 17 keV peak ratios with one standard deviation (STD) for attenuation effects only.

Distance	Point Source		Line 0° Angle		Line 45° Angle		Line 90° Angle	
mm	Ratio	STD	Ratio	STD	Ratio	STD	Ratio	STD
0	1.22	0.17	1.12	0.22	0.68	0.43	1.22	3.05
1.49	0.99	0.15	0.97	0.23	4.43	18.89	-0.04	-0.89
2.34	0.95	0.17	0.63	0.12	0.07	0.25	0.76	0.44
3.83	0.77	0.13	0.72	0.24	-0.62	-0.84	-0.48	-1.15
4.33	0.71	0.13	0.78	0.25	0.22	0.22	1.09	1.41
5.67	0.76	0.14	0.76	0.18	0.05	0.41	-0.12	-0.50
8.01	0.55	0.16	0.45	0.19	0.55	0.91		
10	0.69	0.16	0.80	0.35	-0.78	-0.90		

Combined Effects

Figure 20 shows the peak-to-peak ratio as the sources were moved away from the detector with the distance equal to the thickness of tissue substitute placed between the detector and source. For both of the point and 0° line source the peak-to-peak ratios appear to have a downward trend, but there are noticeable fluctuations across the range. This was due to the lower number of counts in each of the peaks, which adds considerable variability in the ratio. The 45° and 90° source data was omitted once again due to low net counts. Calculated peak-to-peak ratios are tabulated with one standard deviation in table 12.

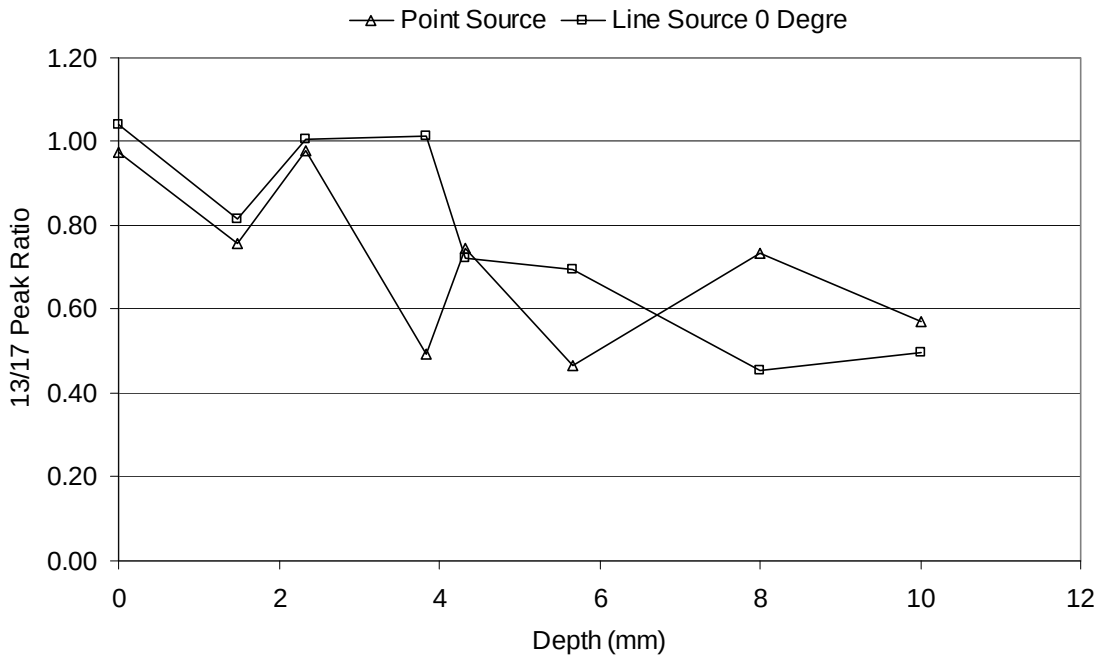

Figure 20: Peak ratio as a function of the combination of distance and attenuation for the point source and the 0° line source orientation.

Table 12: Results of 13 keV to 17keV peak ratios with one standard deviation (STD) for combined distance and attenuation effects.

Distance	Point Source		Line 0° Angle		Line 45° Angle		Line 90° Angle	
mm	Ratio	STD	Ratio	STD	Ratio	STD	Ratio	STD
0	0.98	0.09	1.04	0.11	0.33	0.18	30.33	505.71
1.49	0.76	0.08	0.81	0.11	0.02	0.44	1.20	0.81
2.34	0.98	0.15	1.01	0.18	0.26	0.53	1.18	2.43
3.83	0.50	0.09	1.01	0.24	-9.60	-117.41	-0.54	-3.93
4.33	0.75	0.14	0.72	0.12	0.12	0.57	51.00	2397.29
5.67	0.47	0.11	0.69	0.15			2.24	4.54
8.01	0.73	0.20	0.46	0.18				
10	0.57	0.18	0.50	0.21	0.00	0.78		
14.33	0.04	0.32	0.47	0.30				
20	1.38	2.09	0.96	0.96	-0.86	-1.78		

MCNP RESULTS

NaI(Tl) – Point Source

The MCNP model was used to simulate a point source that was buried increasingly deeper in tissue. This model was similar to the point source experiment, where the source distance was equal to that of the tissue substitute thickness. Results from both experiments have been plotted in figure 21. Mean absolute efficiency from both the experimental data and the model results were close in magnitude and followed the same response curve. The remarkable agreement between the MCNP and experimentally measured efficiencies provides evidence to validate the MCNP model calculation for the NaI(Tl) system.

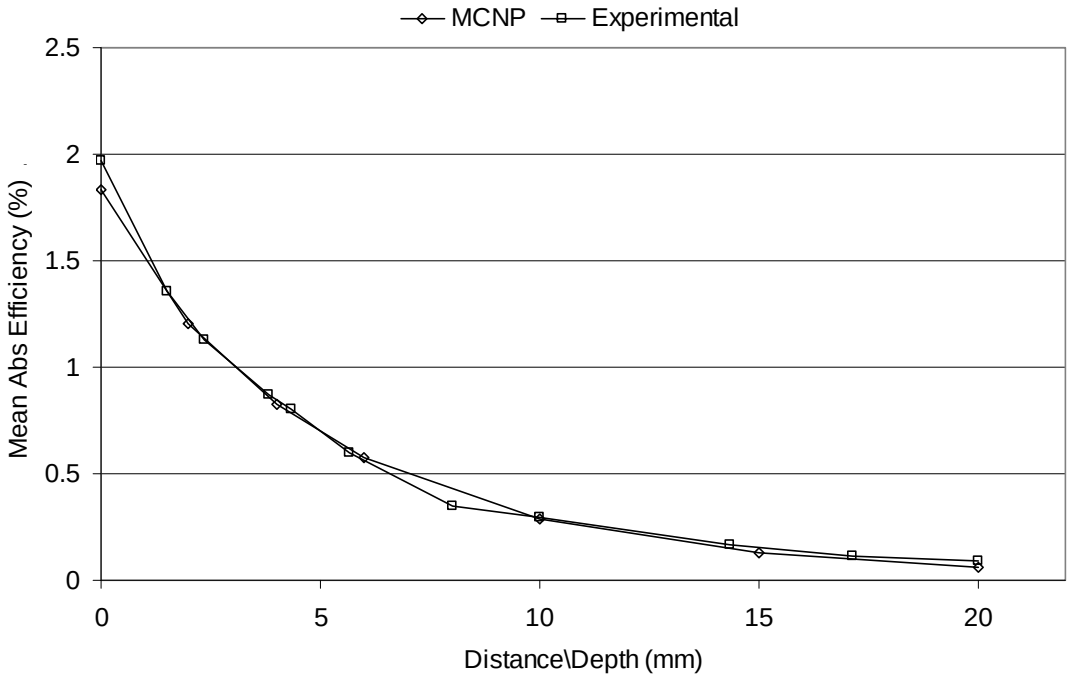

Figure 21: MCNP5 output for a point source moved progressively deeper into tissue.

NaI(Tl) – Line Source

The MCNP code was used to model a line source that was buried in tissue as the source angle with respect to the detector face was increased. The edge of one end of the line source was always placed at a depth of 0.001 cm in the tissue. As the angle of the line source increased, the mean absolute efficiency of the detector decreased. The effect of the angle on detector efficiency was most pronounced for small changes in the angle for angles closer to zero, as shown in figure 22. This means that the greatest uncertainty occurs for linear contamination track wounds with shallow angles.

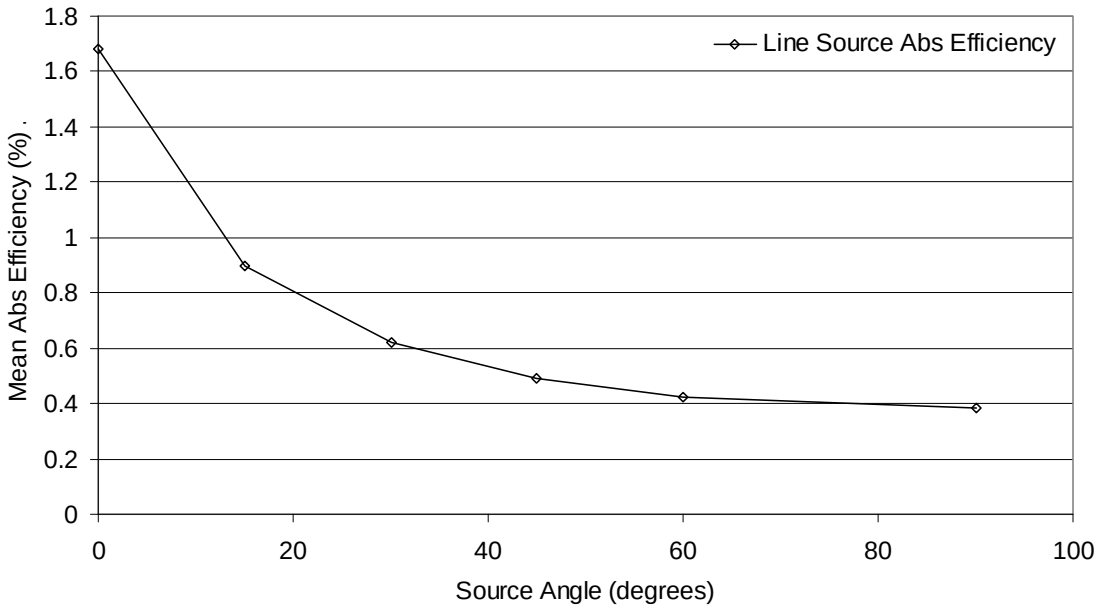

Figure 22: MCNP5 output for a line source in tissue with and increasing incident angle from the detector face.

HPGe – Points Source

The MCNP code was used to model a point source that was buried increasingly deeper in tissue to mimic the experiment in which the point source distance was equal to the tissue substitute thickness. The peak-to-peak ratios from both the experiment and the model results are plotted in figure 23. MCNP peak-to-peak ratio results begin at a lower value and follow a smooth curve of descent, while the experimental results were higher and showed more fluctuation.

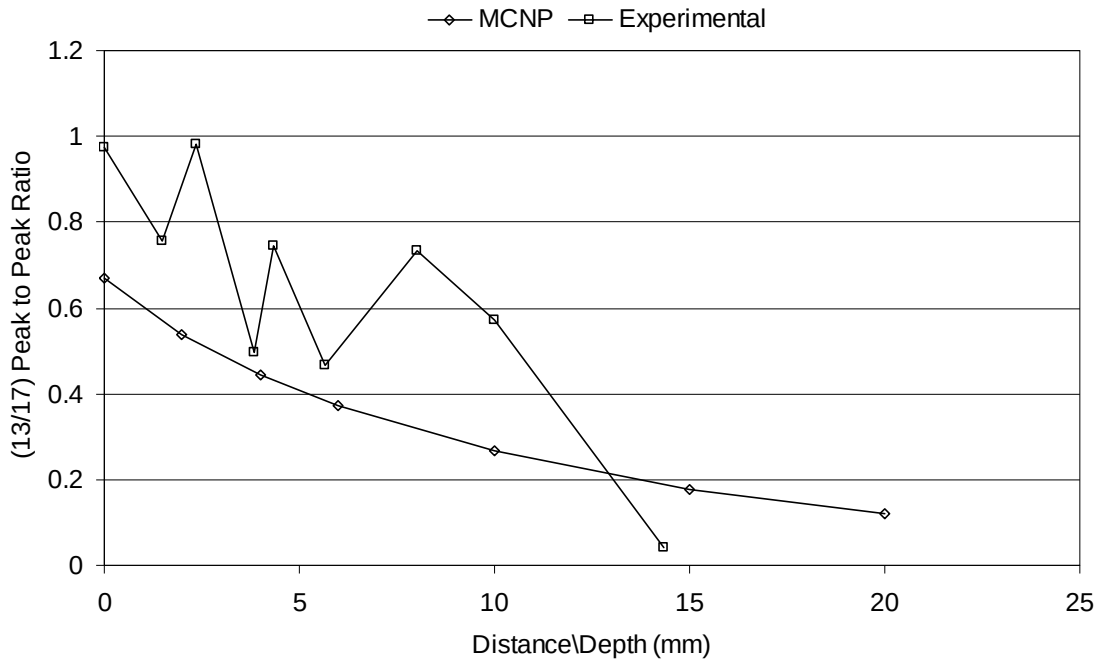

Figure 23: MCNP5 output 13.5 keV peak divided by 17.4 keV peak for a point source embedded progressively deeper in tissue.

HPGe – Line Source

The MCNP code was also used to model a line source that was buried in tissue and oriented at various angles with respect to the detector face. The edge of one side of the line source was set a depth of 0.001 cm in the tissue for all angles. Figure 24 shows the peak-to-peak ratio obtained for six different angles of the line source. As seen in the experimental data, small changes in the angle of the line source close to zero degrees produced more pronounced decreases in the peak-to-peak ratio. After about thirty degrees, small changes in the angle had less of an effect on the peak-to-peak ratio.

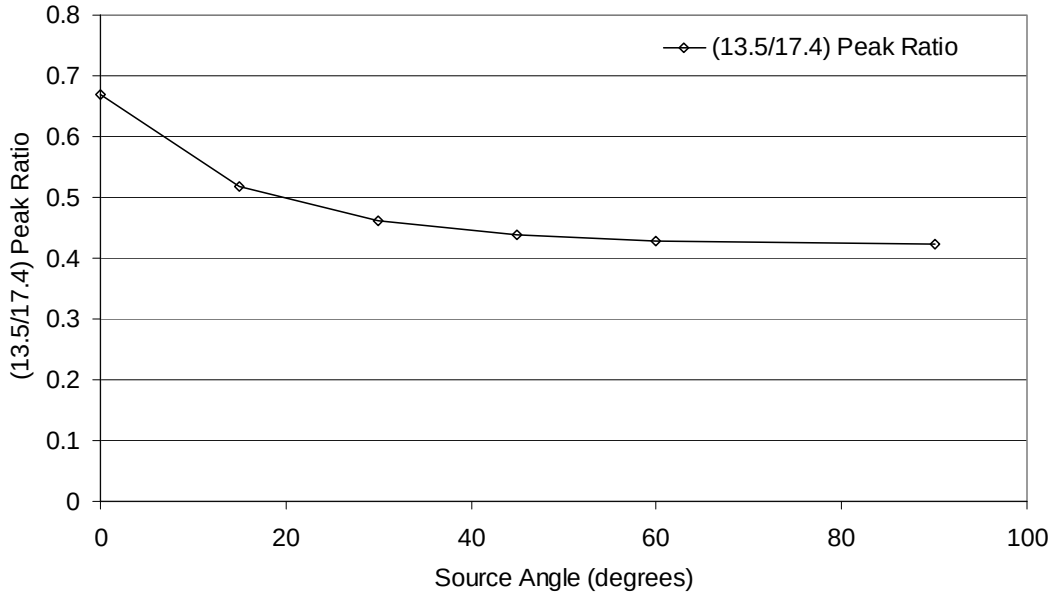

Figure 24: MCNP5 line source output 13.5 keV peak divided by 17.4 keV peak for an increasing incident angle.

CHAPTER IV

CONCLUSION

DISCUSSION

The LANL Health Physics Measurement Group utilizes NaI(Tl) and HPGe detectors to assay the level of plutonium contamination in wounds. Both systems measure the low-energy uranium L-x rays that follow the alpha-particle decay of ^{239}Pu to determine the amount and depth of contamination. The MDA of the NaI(Tl) is between 0.10 to 0.18 nCi, depending on the desired count time, for no attenuation. The NaI(Tl) MDA is 10 to 18 percent of the excision action limit of 1 nCi (Faust et al. 1988). The MDA of the HPGe system was calculated to be about 0.36 nCi, with no attenuation, which is 36 percent of the action limit. Since the MDA of both systems is less than the excision action limit, these are valuable instruments for assessing wound contamination and helping guide medical decisions.

The mean absolute efficiency of the NaI(Tl) system was found to be strongly dependent on source geometry type, distance from the detector, and depth in tissue. Counting efficiencies were generally similar for the disk, point, and line 0° sources and supports the assumption that wounds with these geometries that the counting efficiency determined with a point source is sufficient. But, when the angle of the line source relative to the plane of the detector face was increased, low efficiencies were observed with little effect due to distance and depth in tissue.

The combined effects of distance and attenuation caused the mean absolute detector efficiency to drop below 0.3 percent at a tissue substitute depth of 10 mm. This was an important characteristic of the detector to consider in the assessment of a wound because it suggested the difficulty in accurately measuring contamination at depths greater than 10 mm. This will be difficult to overcome and will require long count times, which may be difficult and uncomfortable for the patient, especially in cases where the activity in the wound is low.

Due to the complications and cost involved with the construction of physical line sources and phantom geometries, MCNP was used to model the NaI(Tl) efficiency response as a function of angle. Results showed that the angle of the source had a substantial effect out to about 45° where the efficiency dropped below 0.5 percent. Beyond 45°, the efficiency response of the detector was not changed much by increasing the angle. Comparison of the point source tissue depth data with the MCNP model provided strong confidence that MCNP was a valid tool for predicting NaI(Tl) detector efficiency for wound geometries that approximate point sources.

Peak-to-peak ratios calculated using the HPGe experimental results changed little with increased source to detector distance. The peak-to-peak ratios showed a downward trend when the source was buried in tissue, similar to what should have been expected due to the increased attenuation of lower-energy photons. Measurements with the HPGe detection system showed large uncertainties when measuring line sources held at angles greater than 0^{o} with respect to the plane of the detector face. This result was due to relatively low activity of the source used in the experiment, low counting efficiencies, and shorter counting times. Counting of high-angle wounds, especially at low activities, will require long count times to reduce the relative error.

Use of the MCNP code to model the detector peak-to-peak ratio response as a function of the source depth in tissue provided some confidence in its application to accurately model wounds. Though, under predicting the magnitude of the ratio for all angles, the model produced results that were on the same order-of-magnitude of the experimental result. Both experimental and MCNP results showed a gradual decreasing slope with increased depth. MCNP was used to model the more complex geometries of a true line source with an increasing angle incident to the plane of the detector face. The peak-to-peak ratio decreased up to angles of 30°, after which the ratio became relatively constant.

Assuming that wound contamination can be approximated as a point source, the results from both detection systems could be utilized to make a more accurate assessment of a single wound. The HPGe system could be used to analyze the wound,

utilizing the peak-to-peak ratio of the 13 keV and 17 keV photopeaks, if a long count time was used. This ratio could then be used to approximate the average depth of contamination using the experimentally determined relationship between the peak-to-peak ratio and the point source depth. The wound could then be measured using the NaI(Tl) system, which will provide net counts of the low-energy x rays. Efficiency of the detection system will be known as a function of point source depth in tissue, which was determined using the HPGe detector. Using the efficiency and the counts in the ROI from the NaI(Tl) system, the total amount of contamination in the wound can be calculated for a particular wound geometry. As the contamination depth approaches 10 mm the measurement of the wound will require a longer count time to achieve an accurate result.

From an operation health physics standpoint, the NaI(Tl) detector is the primary detection system for wound counting. When a wound does occur, the NaI detector system is used to locate and identify contamination in the wound and help guide the medical staff with treatment options. When possible, making the assumption that the wound is a point source and not buried in tissue allows the operator to quickly estimate the amount of material that might be in the wound. The assumption that the material is not buried in tissue actually underestimates the amount of contamination that might exist. Depending on the specifics of the wound, health physics staff can apply an attenuation correction factor based on an assumed depth to provide a more conservative estimate of the activity in the wound. Better accuracy can in some cases be obtained by measurements of burial depth using the HPGe detector system.

In the event the wound geometry is more complicated, the material is deep in tissue, or excision is not practical due to the location of some of the contamination, the HPGe system might be used to try and gain information on the depth of the contamination. Using longer counts times, it might be possible to create an approximate three-dimensional map of the wound to guide excision. Lastly, in the event that the material has to be left in the wound, the HPGe system will be used to create a correction factor to compensate for the attenuation to improve the calculated amount of residual

material in the body. This estimated amount of material that will be left in the body will be used to calculate the expected dose that individual will receive for this intake.

FUTURE WORK

Using the HPGe system to measure contamination in the wound and calculate the peak-to-peak ratio for unfavorable counting geometries was problematic during these experiments. High error from low count rates suggest that the count time used during the measurement should be increased from 1000 seconds. Although, the count time of the measurement cannot be increased much because it would be uncomfortable for a patient to remain motionless for more than 2000 to 3000 seconds. Experimentally, it would be important to redo the experiment of the combined effects of distance and attenuation for a point source using progressively longer count times for the unfavorable geometries. Hopefully, these longer count times would result in a better understanding of the relationships between the peak-to-peak ratios and depth of contamination.

The GLP HPGe detector used for the measurements was one of the original Ortec low-energy spectrometers and may be outdated. Significant advancements in detector crystals, crystal geometries, and counting systems have been made since that time. If possible, some of the simple experiments, such as the point source combined with distance and tissue depth measurement using a newer system with up to date electronics, should be conducted

Finally, it would be useful to create a more complex and accurate MCNP model of other wound geometries that may occur. Wounds are seldom of uniform geometry due to the nature of puncturing and tearing of tissue. It would be useful to create a model to examine the effect of NaI(Tl) detector efficiency for wounds of varying sizes and odd-shaped geometries. Another useful MCNP model would involve imbedding the source in the tissue of a more complex voxelized extremity, such as a hand, and placing the detector as it would be held during an actual wound assessment.

REFERENCES

Attix FH. Introduction to radiological physics and radiation dosimetry. Weinheim: Wiley-VCH; 2004.

Bailey BR, Eckerman KF, Townsend LW. An analysis of a puncture wound case with medical intervention. Radiation Protection Dosimetry 105: 509-512; 2003.

Carbaugh EH, Decker WA, Swint MJ. Medical and health physics management of a plutonium wound. Radiation Protection Dosimetry 26: 345-349; 1989.

Cantwell C, Conner H, Cook S, Hardy M, Hoovler G, William L, McQuinn R, Wannigman D. LANL investigation report: Investigation of two separate worker injuries and resultant internal contamination. Los Alamos National Laboratory Report LA-UR-07-1305; 2007.

DC: U.S. Government Printing Office; 10 CFR Parts 820 and 835; 2007.

Exploring the Table of Isotopes. The Berkeley Laboratory Isotopes Projects'. Available at: http://ie.lbl.gov/education/isotopes.htm. Accessed 14 September 2007.

Faust LG, Brackenbush LW, Heid KR, Herrington WN, Kenoyer JL, Munson LF, Munson LH, Selby JM, Soldat KL, Stoetzel GA, Traub RJ. Health physics manual of good practices for plutonium facilities. Pacific Northwest Laboratory Report PNL-6534/UC-41; 1988.

Guilmette RA, Burbin PW. Scientific basis for the development of biokinetic models for radionuclide-contaminated wounds. Radiation Protection Dosimetry 105: 213-218; 2003.

Hickman DP, Kruchten DA, Fisher SK, Anderson AL. Calibration of a ^{241}Am wound monitoring system using monte carlo techniques. Health Physics 66: 400-406; 1994.

International Commission of Radiation Protection (ICRP). Limits for intake of radionuclides by workers. Oxford, U.K.: Pergamon Press; ICRP Publication 30, Part 1; Ann ICRP 2(3/4): 1979.

International Commission of Radiation Protection (ICRP). Limits for intake of radionuclides by workers. Oxford, U.K.: Pergamon Press; ICRP Publication 38; Ann ICRP 2(3/4): 1983.

International Commission of Radiation Protection (ICRP). Age-dependent doses to members of the public from intake of radionuclides. Oxford, U.K.: Pergamon Press; ICRP Publication 67, Part 2: Ann ICRP 23(3/4): 1987.

International Commission of Radiation Protection (ICRP). Individual monitoring for internal exposure of workers. Oxford, U.K.: Pergamon Press: ICRP Publication 78: Ann ICRP 27(3/4): 1997.

International Commission on Radiation Units and Measurements (ICRU). Tissue substitutes in radiation dosimetry and measurement. Bethesda, MD: ICRU Publication 44: 1989.

Johnson LJ, Lawrence JNP. Plutonium contaminated wound experience and assay techniques at the Los Alamos Scientific Laboratory. Health Physics 27: 55-59; 1974.

Knoll GF. Radiation Detection and Measurement, 3rd ed. New York: Wiley & Sons; 1999.

National Council on Radiation Protection and Measurements. Management of persons accidentally contaminated with radionuclides. Bethesda, MD: NCRP Rep# 65: 1992.

Ortec. GammaVision™ -32 Software user's manual A66-B32. TN: Ametek; 2006.

Ortec. ScintiVision™ -32 Software user's manual A35-B32. TN: Ametek; 2003.

Vasilik DG, Martin RW, Umbarger CJ. A sensitive yet simple plutonium wound monitor. Health Physics 35: 577-578; 1978.

APPENDIX A

NaI(Tl) INPUT DECKS

Point Source 0 mm Depth in Tissue

```
Point Source 0mm depth in tissue
c
c Cell Cards
c ************************************************
c **********************Detector********************
c *****Aluminum Window***********
101 2 -2.7 -102 imp:p=1
c
c *****NaI Crystal***************
102 1 -3.67 -103 imp:p=1
c
c *****PMT Window****************
103 3 -2.33 -104 imp:p=1
c
c *****PMT Volume****************
104 4 -1.22e-3 -105 imp:p=1
c
c *****Aluminum Detector Case****
105 5 -2.7 -106 (101 102 103 104 105) imp:p=1
c
c *****Air Below Entrance Window**
120 6 -1.22e-3 -101 imp:p=1
c
c ****Tissue*********************
201 7 -1 -201 imp:p=1
c
c ********************Inside Universe (air)***********
900 6 -1.22e-3 106 201 -900 imp:p=1
c
c ********************Outside Universe****************
903 0 900 imp:p=0

c
c Surface Cards
c ************************************************
c **********************Detector********************
101 RCC 0 0 0        0 0 0.1600   1.42875
```

```
102 RCC 0 0 0.1600   0 0 0.0025   1.42875
103 RCC 0 0 0.1625   0 0 0.1000   1.3
104 RCC 0 0 0.2625   0 0 0.40165  1.42875
105 RCC 0 0 0.66415  0 0 18.23255  2.0726
106 RCC 0 0 0        0 0 19.05    2.225
107 pz 0.160
c **********************Tissue***********
201 RPP -3.81 3.81 -3.81 3.81 -3.1 -0.01
c **********************Universe Boundary*************
900 RPP -8 8 -8 8 -15 25

c
c Data Cards
c ***************************************************
mode p
c *****NaI************************
c $ NaI (ignoring thallium doping (Hickman))
m1 11000 -0.1534 53000 -0.8466
c
c *****Detector Aluminum window***
m2 13000 1
c
c *****PMT Window*****************
m3 14000 1
c
c *****PMT volume (model as air)
m4 7000 -0.755 8000 -0.232 18000 -0.013
c
c *****Aluminum *****************
m5 13000 1
c
c *****Dry Air*******************
m6 7000 -0.7809 8000 -0.2095 18000 -0.0096
c
c *****Tissue*********************ICRU 44 Adipose
m7     1000 -.114 6000 -.598 7000 -.007 8000 -.278 11000 -.001
       16000 -.001 17000 -.001
C
c ******************Source Definition Cards************
sdef par=2 erg=d1 x=0 y=0 z=-0.02
si1 L 0.01162
     0.013442
     0.013618
     0.0154
```

```
     0.015727
     0.01641
     0.016577
     0.017068
     0.017222
     0.017454
     0.020169
     0.020487
     0.020715
     0.020844
     0.093844
     0.094654
     0.098434
     0.110421
     0.111298
     0.111964
     0.114445
     0.114844
sp1 d 0.023110845
     0.038154697
     0.342302136
     0.009157127
     0.006453594
     0.089391004
     0.010029235
     0.018968335
     0.342302136
     0.009157127
     0.082850199
     0.00414251
     0.003924483
     0.017442147
     0.00000268173
     0.000763094
     0.001242753
     0.000152619
     0.000289976
     0.0000106833
     0.000113374
     0.0000392448
c
c **********TALLY**********
c Tally on NAI crystal
f8:p 102
```

```
e8 0.0001 95i 0.120 $ 1.252 resolution Energy bins
c FT8 is a Gaussian energy Broadening treatment for tally 8
c a,b,c parameters apply to a nominal NAI(Tl) detector
FT8 GEB -0.0137 0.0752 -0.121
c
c ********************Number of particles**************
nps 50000000
```

Point Source 2 mm Depth in Tissue

```
Point Source 2mm depth in tissue
c
c Cell Cards
c ***************************************************
c ***********************Detector********************
c *****Aluminum Window***********
101 2 -2.7 -102 imp:p=1
c
c *****NaI Crystal***************
102 1 -3.67 -103 imp:p=1
c
c *****PMT Window****************
103 3 -2.33 -104 imp:p=1
c
c *****PMT Volume****************
104 4 -1.22e-3 -105 imp:p=1
c
c *****Aluminum Detector Case****
105 5 -2.7 -106 (101 102 103 104 105) imp:p=1
c
c *****Air Below Entrance Window**
120 6 -1.22e-3 -101 imp:p=1
c
c ****Tissue*********************
201 7 -1 -201 imp:p=1
c
c ********************Inside Universe (air)***********
900 6 -1.22e-3 106 201 -900 imp:p=1
c
c ********************Outside Universe***************
903 0 900 imp:p=0

c
```

```
c Surface Cards
c ************************************************
c **********************Detector********************
101 RCC 0 0 0        0 0 0.1600   1.42875
102 RCC 0 0 0.1600   0 0 0.0025   1.42875
103 RCC 0 0 0.1625   0 0 0.1000   1.3
104 RCC 0 0 0.2625   0 0 0.40165  1.42875
105 RCC 0 0 0.66415  0 0 18.23255  2.0726
106 RCC 0 0 0        0 0 19.05    2.225
107 pz 0.160
c **********************Tissue***********
201 RPP -3.81 3.81 -3.81 3.81 -3.1 -0.01
c **********************Universe Boundary*************
900 RPP -8 8 -8 8 -15 25

c
c Data Cards
c ************************************************
mode p
c *****NaI************************
m1 11000 -0.1534 53000 -0.8466
c  NaI (ignoring thallium doping (Hickman))
c
c *****Detector Aluminum window***
m2 13000 1
c
c *****PMT Window*****************
m3 14000 1
c
c *****PMT volume (model as  air)
m4 7000 -0.755 8000 -0.232 18000 -0.013
c
c *****Aluminum ******************
m5 13000 1
c
c *****Dry Air*********************
m6 7000 -0.7809 8000 -0.2095 18000 -0.0096
c
c *****Tissue**********************ICRU 44 Adipose
m7     1000 -.114 6000 -.598 7000 -.007 8000 -.278 11000 -.001
       16000 -.001 17000 -.001
C
c ******************Source Definition Cards************
sdef par=2 erg=d1 x=0 y=0 z=-0.22
```

si1 L 0.01162
0.013442
0.013618
0.0154
0.015727
0.01641
0.016577
0.017068
0.017222
0.017454
0.020169
0.020487
0.020715
0.020844
0.093844
0.094654
0.098434
0.110421
0.111298
0.111964
0.114445
0.114844
sp1 d 0.023110845
0.038154697
0.342302136
0.009157127
0.006453594
0.089391004
0.010029235
0.018968335
0.342302136
0.009157127
0.082850199
0.00414251
0.003924483
0.017442147
0.00000268173
0.000763094
0.001242753
0.000152619
0.000289976
0.0000106833
0.000113374
0.0000392448

```
c
c **********************TALLY*************************
c Tally on NAI crystal
f8:p 102
e8 0.0001 95i 0.120 $ 1.252 resolution Energy bins
c FT8 is a Gaussian energy Broadening treatment for tally 8
c a,b,c parameters apply to a nominal NAI(Tl) detector
FT8 GEB -0.0137 0.0752 -0.121
c
c **********************Number of particles***************
nps 50000000
```

Point Source 4 mm Depth in Tissue

```
Point source 4mm depth in tissue
c
c Cell Cards
c ***************************************************
c **********************Detector*********************
c *****Aluminum Window***********
101 2 -2.7 -102 imp:p=1
c
c *****NaI Crystal***************
102 1 -3.67 -103 imp:p=1
c
c *****PMT Window****************
103 3 -2.33 -104 imp:p=1
c
c *****PMT Volume****************
104 4 -1.22e-3 -105 imp:p=1
c
c *****Aluminum Detector Case****
105 5 -2.7 -106 (101 102 103 104 105) imp:p=1
c
c *****Air Below Entrance Window**
120 6 -1.22e-3 -101 imp:p=1
c
c ****Tissue*********************
201 7 -1 -201 imp:p=1
c
c ********************Inside Universe (air)***********
```

```
900 6 -1.22e-3 106 201 -900 imp:p=1
c
c ********************Outside Universe***************
903 0 900 imp:p=0

c
c Surface Cards
c ************************************************
c ***********************Detector********************
101 RCC 0 0 0        0 0 0.1600   1.42875
102 RCC 0 0 0.1600   0 0 0.0025   1.42875
103 RCC 0 0 0.1625   0 0 0.1000   1.3
104 RCC 0 0 0.2625   0 0 0.40165  1.42875
105 RCC 0 0 0.66415  0 0 18.23255  2.0726
106 RCC 0 0 0        0 0 19.05    2.225
107 pz 0.160
c ***********************Tissue***********
201 RPP -3.81 3.81 -3.81 3.81 -3.1 -0.01
c ***********************Universe Boundary*************
900 RPP -8 8 -8 8 -15 25

c
c Data Cards
c ************************************************
mode p
c *****NaI************************
m1 11000 -0.1534 53000 -0.8466
c $ NaI (ignoring thallium doping (Hickman))
c
c *****Detector Aluminum window***
m2 13000 1
c
c *****PMT Window*****************
m3 14000 1
c
c *****PMT volume (model as air)
m4 7000 -0.755 8000 -0.232 18000 -0.013
c
c *****Aluminum ******************
m5 13000 1
c
c *****Dry Air********************
m6 7000 -0.7809 8000 -0.2095 18000 -0.0096
c
```

```
c *****Tissue**********************ICRU 44 Adipose
m7     1000 -.114 6000 -.598 7000 -.007 8000 -.278 11000 -.001
       16000 -.001 17000 -.001
C
c ******************Source Definition Cards************
sdef par=2 erg=d1 x=0 y=0 z=-0.42
si1 L 0.01162
     0.013442
     0.013618
     0.0154
     0.015727
     0.01641
     0.016577
     0.017068
     0.017222
     0.017454
     0.020169
     0.020487
     0.020715
     0.020844
     0.093844
     0.094654
     0.098434
     0.110421
     0.111298
     0.111964
     0.114445
     0.114844
sp1 d 0.023110845
     0.038154697
     0.342302136
     0.009157127
     0.006453594
     0.089391004
     0.010029235
     0.018968335
     0.342302136
     0.009157127
     0.082850199
     0.00414251
     0.003924483
     0.017442147
     0.00000268173
     0.000763094
```

```
     0.001242753
     0.000152619
     0.000289976
     0.0000106833
     0.000113374
     0.0000392448
c
c **********************TALLY**************************
c Tally on NAI crystal
f8:p 102
e8 0.0001 95i 0.120 $ 1.252 resolution Energy bins
c FT8 is a Gaussian energy Broadening treatment for tally 8
c a,b,c parameters apply to a nominal NAI(Tl) detector
FT8 GEB -0.0137 0.0752 -0.121
c
c **********************Number of particles***************
nps 50000000
```

Point Source 6 mm Depth in Tissue

```
Point Source 6mm depth in tissue
c
c Cell Cards
c ***************************************************
c **********************Detector*********************
c *****Aluminum Window***********
101 2 -2.7 -102 imp:p=1
c
c *****NaI Crystal***************
102 1 -3.67 -103 imp:p=1
c
c *****PMT Window****************
103 3 -2.33 -104 imp:p=1
c
c *****PMT Volume****************
104 4 -1.22e-3 -105 imp:p=1
c
c *****Aluminum Detector Case****
105 5 -2.7 -106 (101 102 103 104 105) imp:p=1
c
c *****Air Below Entrance Window**
```

```
120 6 -1.22e-3 -101 imp:p=1
c
c ****Tissue*********************
201 7 -1 -201 imp:p=1
c
c ********************Inside Universe (air)***********
900 6 -1.22e-3 106 201 -900 imp:p=1
c
c ********************Outside Universe***************
903 0 900 imp:p=0

c
c Surface Cards
c ************************************************
c ************************Detector********************
101 RCC 0 0 0        0 0 0.1600   1.42875
102 RCC 0 0 0.1600   0 0 0.0025   1.42875
103 RCC 0 0 0.1625   0 0 0.1000   1.3
104 RCC 0 0 0.2625   0 0 0.40165  1.42875
105 RCC 0 0 0.66415  0 0 18.23255  2.0726
106 RCC 0 0 0        0 0 19.05    2.225
107 pz 0.160
c ************************Tissue***********
201 RPP -3.81 3.81 -3.81 3.81 -3.1 -0.01
c ************************Universe Boundary*************
900 RPP -8 8 -8 8 -15 25

c
c Data Cards
c ************************************************
mode p
c *****NaI************************
m1 11000 -0.1534 53000 -0.8466
c $ NaI (ignoring thallium doping (Hickman))
c
c *****Detector Aluminum window***
m2 13000 1
c
c *****PMT Window*****************
m3 14000 1
c
c *****PMT volume (model as air)
m4 7000 -0.755 8000 -0.232 18000 -0.013
c
```

```
c *****Aluminum ****************
m5 13000 1
c
c *****Dry Air*******************
m6 7000 -0.7809 8000 -0.2095 18000 -0.0096
c
c *****Tissue*********************ICRU 44 Adipose
m7     1000 -.114 6000 -.598 7000 -.007 8000 -.278 11000 -.001
       16000 -.001 17000 -.001
C
c ******************Source Definition Cards************
sdef par=2 erg=d1 x=0 y=0 z=-0.62
si1 L 0.01162
      0.013442
      0.013618
      0.0154
      0.015727
      0.01641
      0.016577
      0.017068
      0.017222
      0.017454
      0.020169
      0.020487
      0.020715
      0.020844
      0.093844
      0.094654
      0.098434
      0.110421
      0.111298
      0.111964
      0.114445
      0.114844
sp1 d 0.023110845
      0.038154697
      0.342302136
      0.009157127
      0.006453594
      0.089391004
      0.010029235
      0.018968335
      0.342302136
      0.009157127
```

```
     0.082850199
     0.00414251
     0.003924483
     0.017442147
     0.00000268173
     0.000763094
     0.001242753
     0.000152619
     0.000289976
     0.0000106833
     0.000113374
     0.0000392448
c
c **********************TALLY*************************
c Tally on NAI crystal
f8:p 102
e8 0.0001 95i 0.120 $ 1.252 resolution Energy bins
c FT8 is a Gaussian energy Broadening treatment for tally 8
c a,b,c parameters apply to a nominal NAI(Tl) detector
FT8 GEB -0.0137 0.0752 -0.121
c
c **********************Number of particles***************
nps 50000000
```

Point Source 10 mm Depth in Tissue

```
Point source 10mm depth in tissue
c
c Cell Cards
c ***************************************************
c ***********************Detector*********************
c *****Aluminum Window***********
101 2 -2.7 -102 imp:p=1
c
c *****NaI Crystal***************
102 1 -3.67 -103 imp:p=1
c
c *****PMT Window****************
103 3 -2.33 -104 imp:p=1
c
c *****PMT Volume****************
```

```
104 4 -1.22e-3 -105 imp:p=1
c
c *****Aluminum Detector Case****
105 5 -2.7 -106 (101 102 103 104 105) imp:p=1
c
c *****Air Below Entrance Window**
120 6 -1.22e-3 -101 imp:p=1
c
c ****Tissue*********************
201 7 -1 -201 imp:p=1
c
c ********************Inside Universe (air)***********
900 6 -1.22e-3 106 201 -900 imp:p=1
c
c ********************Outside Universe***************
903 0 900 imp:p=0

c
c Surface Cards
c ***************************************************
c ***********************Detector*********************
101 RCC 0 0 0        0 0 0.1600   1.42875
102 RCC 0 0 0.1600   0 0 0.0025   1.42875
103 RCC 0 0 0.1625   0 0 0.1000   1.3
104 RCC 0 0 0.2625   0 0 0.40165  1.42875
105 RCC 0 0 0.66415  0 0 18.23255  2.0726
106 RCC 0 0 0        0 0 19.05    2.225
107 pz 0.160
c ***********************Tissue***********
201 RPP -3.81 3.81 -3.81 3.81 -3.1 -0.01
c ***********************Universe Boundary*************
900 RPP -8 8 -8 8 -15 25

c
c Data Cards
c ***************************************************
mode p
c *****NaI************************
m1 11000 -0.1534 53000 -0.8466
c $ NaI (ignoring thallium doping (Hickman))
c
c *****Detector Aluminum window***
m2 13000 1
c
```

```
c *****PMT Window*****************
m3 14000 1
c
c *****PMT volume (model air)
m4 7000 -0.755 8000 -0.232 18000 -0.013
c
c *****Aluminum *****************
m5 13000 1
c
c *****Dry Air*******************
m6 7000 -0.7809 8000 -0.2095 18000 -0.0096
c
c *****Tissue*********************ICRU 44 Adipose
m7     1000 -.114 6000 -.598 7000 -.007 8000 -.278 11000 -.001
       16000 -.001 17000 -.001
C
c ******************Source Definition Cards************
sdef par=2 erg=d1 x=0 y=0 z=-1.02
si1 L 0.01162
     0.013442
     0.013618
     0.0154
     0.015727
     0.01641
     0.016577
     0.017068
     0.017222
     0.017454
     0.020169
     0.020487
     0.020715
     0.020844
     0.093844
     0.094654
     0.098434
     0.110421
     0.111298
     0.111964
     0.114445
     0.114844
sp1 d 0.023110845
     0.038154697
     0.342302136
     0.009157127
```

```
     0.006453594
     0.089391004
     0.010029235
     0.018968335
     0.342302136
     0.009157127
     0.082850199
     0.00414251
     0.003924483
     0.017442147
     0.00000268173
     0.000763094
     0.001242753
     0.000152619
     0.000289976
     0.0000106833
     0.000113374
     0.0000392448
c
c **********************TALLY*************************
c Tally on NAI crystal
f8:p 102
e8 0.0001 95i 0.120 $ 1.252 resolution Energy bins
c FT8 is a Gaussian energy Broadening treatment for tally 8
c a,b,c parameters apply to a nominal NAI(Tl) detector
FT8 GEB -0.0137 0.0752 -0.121
c
c **********************Number of particles***************
nps 50000000
```

Point Source 15 mm Depth in Tissue

```
Point source 15mm depth in tissue
c
c Cell Cards
c ***************************************************
c **********************Detector*********************
c *****Aluminum Window***********
101 2 -2.7 -102 imp:p=1
c
c *****NaI Crystal***************
```

```
102 1 -3.67 -103 imp:p=1
c
c *****PMT Window***************
103 3 -2.33 -104 imp:p=1
c
c *****PMT Volume***************
104 4 -1.22e-3 -105 imp:p=1
c
c *****Aluminum Detector Case****
105 5 -2.7 -106 (101 102 103 104 105) imp:p=1
c
c *****Air Below Entrance Window**
120 6 -1.22e-3 -101 imp:p=1
c
c ****Tissue*********************
201 7 -1 -201 imp:p=1
c
c ********************Inside Universe (air)***********
900 6 -1.22e-3 106 201 -900 imp:p=1
c
c ********************Outside Universe***************
903 0 900 imp:p=0

c
c Surface Cards
c ***************************************************
c ***********************Detector********************
101 RCC 0 0 0        0 0 0.1600   1.42875
102 RCC 0 0 0.1600   0 0 0.0025   1.42875
103 RCC 0 0 0.1625   0 0 0.1000   1.3
104 RCC 0 0 0.2625   0 0 0.40165  1.42875
105 RCC 0 0 0.66415  0 0 18.23255  2.0726
106 RCC 0 0 0        0 0 19.05    2.225
107 pz 0.160
c ***********************Tissue***********
201 RPP -3.81 3.81 -3.81 3.81 -3.1 -0.01
c ***********************Universe Boundary*************
900 RPP -8 8 -8 8 -15 25

c
c Data Cards
c ***************************************************
mode p
c *****NaI************************
```

```
m1 11000 -0.1534 53000 -0.8466
c $ NaI (ignoring thallium doping (Hickman))
c
c *****Detector Aluminum window***
m2 13000 1
c
c *****PMT Window*****************
m3 14000 1
c
c *****PMT volume (model as dry air for now 5/24/07)
m4 7000 -0.755 8000 -0.232 18000 -0.013
c
c *****Aluminum *****************
m5 13000 1
c
c *****Dry Air*******************
m6 7000 -0.7809 8000 -0.2095 18000 -0.0096
c
c *****Tissue*********************ICRU 44 Adipose
m7     1000 -.114 6000 -.598 7000 -.007 8000 -.278 11000 -.001
      16000 -.001 17000 -.001
C
c ******************Source Definition Cards************
sdef par=2 erg=d1 x=0 y=0 z=-1.52
si1 L 0.01162
     0.013442
     0.013618
     0.0154
     0.015727
     0.01641
     0.016577
     0.017068
     0.017222
     0.017454
     0.020169
     0.020487
     0.020715
     0.020844
     0.093844
     0.094654
     0.098434
     0.110421
     0.111298
     0.111964
```

```
     0.114445
     0.114844
sp1 d 0.023110845
     0.038154697
     0.342302136
     0.009157127
     0.006453594
     0.089391004
     0.010029235
     0.018968335
     0.342302136
     0.009157127
     0.082850199
     0.00414251
     0.003924483
     0.017442147
     0.00000268173
     0.000763094
     0.001242753
     0.000152619
     0.000289976
     0.0000106833
     0.000113374
     0.0000392448
c
c **********************TALLY*************************
c Tally on NAI crystal
f8:p 102
e8 0.0001 95i 0.120 $ 1.252 resolution Energy bins
c FT8 is a gaussian energy Broadening treatment for tally 8
c a,b,c parameters apply to a nominal NAI(Tl) detector
FT8 GEB -0.0137 0.0752 -0.121
c
c **********************Number of particles***************
nps 50000000
```

Point Source 20 mm Depth in Tissue

```
Point source 20mm depth in tissue
c
c Cell Cards
```

```
c ***************************************************
c **********************Detector*********************
c *****Aluminum Window***********
101 2 -2.7 -102 imp:p=1
c
c *****NaI Crystal***************
102 1 -3.67 -103 imp:p=1
c
c *****PMT Window****************
103 3 -2.33 -104 imp:p=1
c
c *****PMT Volume****************
104 4 -1.22e-3 -105 imp:p=1
c
c *****Aluminum Detector Case****
105 5 -2.7 -106 (101 102 103 104 105) imp:p=1
c
c *****Air Below Entrance Window**
120 6 -1.22e-3 -101 imp:p=1
c
c ****Tissue*********************
201 7 -1 -201 imp:p=1
c
c ********************Inside Universe (air)***********
900 6 -1.22e-3 106 201 -900 imp:p=1
c
c ********************Outside Universe****************
903 0 900 imp:p=0

c
c Surface Cards
c ***************************************************
c **********************Detector*********************
101 RCC 0 0 0        0 0 0.1600   1.42875
102 RCC 0 0 0.1600   0 0 0.0025   1.42875
103 RCC 0 0 0.1625   0 0 0.1000   1.3
104 RCC 0 0 0.2625   0 0 0.40165  1.42875
105 RCC 0 0 0.66415  0 0 18.23255  2.0726
106 RCC 0 0 0        0 0 19.05    2.225
107 pz 0.160
c **********************Tissue***********
201 RPP -3.81 3.81 -3.81 3.81 -3.1 -0.01
c **********************Universe Boundary*************
900 RPP -8 8 -8 8 -15 25
```

```
c
c Data Cards
c ***************************************************
mode p
c *****NaI***********************
m1 11000 -0.1534 53000 -0.8466
c $ NaI (ignoring thallium doping (Hickman))
c
c *****Detector Aluminum window***
m2 13000 1
c
c *****PMT Window*****************
m3 14000 1
c
c *****PMT volume (model as air)
m4 7000 -0.755 8000 -0.232 18000 -0.013
c
c *****Aluminum *****************
m5 13000 1
c
c *****Dry Air*******************
m6 7000 -0.7809 8000 -0.2095 18000 -0.0096
c
c *****Tissue*********************ICRU 44 Adipose
m7     1000 -.114 6000 -.598 7000 -.007 8000 -.278 11000 -.001
       16000 -.001 17000 -.001
C
c ******************Source Definition Cards************
sdef par=2 erg=d1 x=0 y=0 z=-2.02
si1 L 0.01162
     0.013442
     0.013618
     0.0154
     0.015727
     0.01641
     0.016577
     0.017068
     0.017222
     0.017454
     0.020169
     0.020487
     0.020715
     0.020844
```

```
     0.093844
     0.094654
     0.098434
     0.110421
     0.111298
     0.111964
     0.114445
     0.114844
sp1 d 0.023110845
     0.038154697
     0.342302136
     0.009157127
     0.006453594
     0.089391004
     0.010029235
     0.018968335
     0.342302136
     0.009157127
     0.082850199
     0.00414251
     0.003924483
     0.017442147
     0.00000268173
     0.000763094
     0.001242753
     0.000152619
     0.000289976
     0.0000106833
     0.000113374
     0.0000392448
c
c **********************TALLY*************************
c Tally on NAI crystal
f8:p 102
e8 0.0001 95i 0.120 $ 1.252 resolution Energy bins
c FT8 is a Gaussian energy Broadening treatment for tally 8
c a,b,c parameters apply to a nominal NAI(Tl) detector
FT8 GEB -0.0137 0.0752 -0.121
c
c **********************Number of particles**************
nps 50000000
```

Line Source 0° Incident Angle

```
Line source 0 degree incident angle
c
c Cell Cards
c ***************************************************
c **********************Detector*********************
c *****Aluminum Window***********
101 2 -2.7 -102 imp:p=1
c
c *****NaI Crystal***************
102 1 -3.67 -103 imp:p=1
c
c *****PMT Window****************
103 3 -2.33 -104 imp:p=1
c
c *****PMT Volume****************
104 4 -1.22e-3 -105 imp:p=1
c
c *****Aluminum Detector Case****
105 5 -2.7 -106 (101 102 103 104 105) imp:p=1
c
c *****Air Below Entrance Window**
120 6 -1.22e-3 -101 imp:p=1
c
c ****Tissue*********************
201 7 -1 -201 imp:p=1
c
c ********************Inside Universe (air)***********
900 6 -1.22e-3 106 201 -900 imp:p=1
c
c ********************Outside Universe***************
903 0 900 imp:p=0

c
c Surface Cards
c ***************************************************
c **********************Detector*********************
101 RCC 0 0 0        0 0 0.1600   1.42875
102 RCC 0 0 0.1600   0 0 0.0025   1.42875
103 RCC 0 0 0.1625   0 0 0.1000   1.3
104 RCC 0 0 0.2625   0 0 0.40165  1.42875
105 RCC 0 0 0.66415  0 0 18.23255  2.0726
```

```
106 RCC 0 0 0        0 0 19.05    2.225
107 pz 0.160
c **********************Tissue***********
201 RPP -3.81 3.81 -3.81 3.81 -3.1 -0.01
c **********************Universe Boundary*************
900 RPP -8 8 -8 8 -15 25

c
c Data Cards
c ******************************************************
mode p
c *****NaI************************
m1 11000 -0.1534 53000 -0.8466
c $ NaI (ignoring thallium doping (Hickman))
c
c *****Detector Aluminum window***
m2 13000 1
c
c *****PMT Window*****************
m3 14000 1
c
c *****PMT volume (model as air)
m4 7000 -0.755 8000 -0.232 18000 -0.013
c
c *****Aluminum ******************
m5 13000 1
c
c *****Dry Air*********************
m6 7000 -0.7809 8000 -0.2095 18000 -0.0096
c
c *****Tissue**********************ICRU 44 Adipose
m7     1000 -.114 6000 -.598 7000 -.007 8000 -.278 11000 -.001
       16000 -.001 17000 -.001
C
c ******************Source Definition Cards************
sdef par=2 erg=d1 x=0 y=d2 z=-0.02
si2 -1.27 1.27
sp2 0.0 1.0
si1 L 0.01162
     0.013442
     0.013618
     0.0154
     0.015727
     0.01641
```

```
     0.016577
     0.017068
     0.017222
     0.017454
     0.020169
     0.020487
     0.020715
     0.020844
     0.093844
     0.094654
     0.098434
     0.110421
     0.111298
     0.111964
     0.114445
     0.114844
sp1 d 0.023110845
     0.038154697
     0.342302136
     0.009157127
     0.006453594
     0.089391004
     0.010029235
     0.018968335
     0.342302136
     0.009157127
     0.082850199
     0.00414251
     0.003924483
     0.017442147
     0.00000268173
     0.000763094
     0.001242753
     0.000152619
     0.000289976
     0.0000106833
     0.000113374
     0.0000392448
c
c **********************TALLY*************************
c Tally on NAI crystal
f8:p 102
e8 0.0001 95i 0.120 $ 1.252 resolution Energy bins
c FT8 is a Gaussian energy Broadening treatment for tally 8
```

```
c a,b,c parameters apply to a nominal NAI(Tl) detector
FT8 GEB -0.0137 0.0752 -0.121
c
c **********Number of particles**********
nps 50000000
```

Line Source 15° Incident Angle

```
Line source 15 degree incident angle
c
c Cell Cards
c ***************************************************
c **********Detector**********
c *****Aluminum Window**********
101 2 -2.7 -102 imp:p=1
c
c *****NaI Crystal**********
102 1 -3.67 -103 imp:p=1
c
c *****PMT Window**********
103 3 -2.33 -104 imp:p=1
c
c *****PMT Volume**********
104 4 -1.22e-3 -105 imp:p=1
c
c *****Aluminum Detector Case****
105 5 -2.7 -106 (101 102 103 104 105) imp:p=1
c
c *****Air Below Entrance Window**
120 6 -1.22e-3 -101 imp:p=1
c
c ****Tissue**********
201 7 -1 -201 imp:p=1
c
c **********Inside Universe (air)**********
900 6 -1.22e-3 106 201 -900 imp:p=1
c
c **********Outside Universe**********
903 0 900 imp:p=0

c
c Surface Cards
c ***************************************************
```

```
c **********Detector**********
101 RCC 0 0 0        0 0 0.1600   1.42875
102 RCC 0 0 0.1600   0 0 0.0025   1.42875
103 RCC 0 0 0.1625   0 0 0.1000   1.3
104 RCC 0 0 0.2625   0 0 0.40165  1.42875
105 RCC 0 0 0.66415  0 0 18.23255  2.0726
106 RCC 0 0 0        0 0 19.05    2.225
107 pz 0.160
c **********Tissue**********
201 RPP -3.81 3.81 -3.81 3.81 -3.1 -0.01
c **********Universe Boundary**********
900 RPP -8 8 -8 8 -15 25

c
c Data Cards
c **************************************************
mode p
c *****NaI**********
m1 11000 -0.1534 53000 -0.8466
c $ NaI (ignoring thallium doping (Hickman))
c
c *****Detector Aluminum window***
m2 13000 1
c
c *****PMT Window**********
m3 14000 1
c
c *****PMT volume (model as air for)
m4 7000 -0.755 8000 -0.232 18000 -0.013
c
c *****Aluminum **********
m5 13000 1
c
c *****Dry Air**********
m6 7000 -0.7809 8000 -0.2095 18000 -0.0096
c
c *****Tissue**********ICRU 44 Adipose
m7     1000 -.114 6000 -.598 7000 -.007 8000 -.278 11000 -.001
       16000 -.001 17000 -.001
C
c **********Source Definition Cards**********
sdef par=2 erg=d1 x=0 y=d2 z=d3
si2 -1.22673 1.22673
sp2 0.0 1.0
```

si3 -0.6774 -0.02
sp3 0.0 1.0
si1 L 0.01162
0.013442
0.013618
0.0154
0.015727
0.01641
0.016577
0.017068
0.017222
0.017454
0.020169
0.020487
0.020715
0.020844
0.093844
0.094654
0.098434
0.110421
0.111298
0.111964
0.114445
0.114844
sp1 d 0.023110845
0.038154697
0.342302136
0.009157127
0.006453594
0.089391004
0.010029235
0.018968335
0.342302136
0.009157127
0.082850199
0.00414251
0.003924483
0.017442147
0.00000268173
0.000763094
0.001242753
0.000152619
0.000289976
0.0000106833

```
     0.000113374
     0.0000392448
c
c **********************TALLY*************************
c Tally on NAI crystal
f8:p 102
e8 0.0001 95i 0.120 $ 1.252 resolution Energy bins
c FT8 is a Gaussian energy Broadening treatment for tally 8
c a,b,c parameters apply to a nominal NAI(Tl) detector
FT8 GEB -0.0137 0.0752 -0.121
c
c **********************Number of particles***************
nps 50000000
```

Line Source 30° Incident Angle

```
Line source 30 degree incident angle
c
c Cell Cards
c ***************************************************
c **********************Detector*********************
c *****Aluminum Window***********
101 2 -2.7 -102 imp:p=1
c
c *****NaI Crystal***************
102 1 -3.67 -103 imp:p=1
c
c *****PMT Window****************
103 3 -2.33 -104 imp:p=1
c
c *****PMT Volume****************
104 4 -1.22e-3 -105 imp:p=1
c
c *****Aluminum Detector Case****
105 5 -2.7 -106 (101 102 103 104 105) imp:p=1
c
c *****Air Below Entrance Window**
120 6 -1.22e-3 -101 imp:p=1
c
c ****Tissue*********************
201 7 -1 -201 imp:p=1
c
c ********************Inside Universe (air)***********
900 6 -1.22e-3 106 201 -900 imp:p=1
c
```

```
c ********************Outside Universe***************
903 0 900 imp:p=0

c
c Surface Cards
c ************************************************
c ***********************Detector********************
101 RCC 0 0 0        0 0 0.1600   1.42875
102 RCC 0 0 0.1600   0 0 0.0025   1.42875
103 RCC 0 0 0.1625   0 0 0.1000   1.3
104 RCC 0 0 0.2625   0 0 0.40165  1.42875
105 RCC 0 0 0.66415  0 0 18.23255  2.0726
106 RCC 0 0 0        0 0 19.05    2.225
107 pz 0.160
c ***********************Tissue***********
201 RPP -3.81 3.81 -3.81 3.81 -3.1 -0.01
c ***********************Universe Boundary*************
900 RPP -8 8 -8 8 -15 25

c
c Data Cards
c ************************************************
mode p
c *****NaI************************
m1 11000 -0.1534 53000 -0.8466
c $ NaI (ignoring thallium doping (Hickman))
c
c *****Detector Aluminum window***
m2 13000 1
c
c *****PMT Window*****************
m3 14000 1
c
c *****PMT volume (model as air)
m4 7000 -0.755 8000 -0.232 18000 -0.013
c
c *****Aluminum *****************
m5 13000 1
c
c *****Dry Air*********************
m6 7000 -0.7809 8000 -0.2095 18000 -0.0096
c
c *****Tissue**********************ICRU 44 Adipose
m7     1000 -.114 6000 -.598 7000 -.007 8000 -.278 11000 -.001
```

```
      16000 -.001 17000 -.001
C
c ******************Source Definition Cards************
sdef par=2 erg=d1 x=0 y=d2 z=d3
si2 -1.09985 1.09985
sp2 0.0 1.0
si3 -1.29 -0.02
sp3 0.0 1.0
si1 L 0.01162
     0.013442
     0.013618
     0.0154
     0.015727
     0.01641
     0.016577
     0.017068
     0.017222
     0.017454
     0.020169
     0.020487
     0.020715
     0.020844
     0.093844
     0.094654
     0.098434
     0.110421
     0.111298
     0.111964
     0.114445
     0.114844
sp1 d 0.023110845
     0.038154697
     0.342302136
     0.009157127
     0.006453594
     0.089391004
     0.010029235
     0.018968335
     0.342302136
     0.009157127
     0.082850199
     0.00414251
     0.003924483
     0.017442147
```

```
     0.00000268173
     0.000763094
     0.001242753
     0.000152619
     0.000289976
     0.0000106833
     0.000113374
     0.0000392448
c
c **********************TALLY*************************
c Tally on NAI crystal
f8:p 102
e8 0.0001 95i 0.120 $ 1.252 resolution Energy bins
c FT8 is a Gaussian energy Broadening treatment for tally 8
c a,b,c parameters apply to a nominal NAI(Tl) detector
FT8 GEB -0.0137 0.0752 -0.121
c
c **********************Number of particles***************
nps 50000000
```

Line Source 45° Incident Angle

```
Line source 60 degree incident angle
c
c Cell Cards
c ***************************************************
c **********************Detector*********************
c *****Aluminum Window***********
101 2 -2.7 -102 imp:p=1
c
c *****NaI Crystal***************
102 1 -3.67 -103 imp:p=1
c
c *****PMT Window****************
103 3 -2.33 -104 imp:p=1
c
c *****PMT Volume****************
104 4 -1.22e-3 -105 imp:p=1
c
c *****Aluminum Detector Case****
105 5 -2.7 -106 (101 102 103 104 105) imp:p=1
c
c *****Air Below Entrance Window**
120 6 -1.22e-3 -101 imp:p=1
c
```

```
c ****Tissue*********************
201 7 -1 -201 imp:p=1
c
c ********************Inside Universe (air)***********
900 6 -1.22e-3 106 201 -900 imp:p=1
c
c ********************Outside Universe***************
903 0 900 imp:p=0

c
c Surface Cards
c ************************************************
c ***********************Detector********************
101 RCC 0 0 0        0 0 0.1600   1.42875
102 RCC 0 0 0.1600   0 0 0.0025   1.42875
103 RCC 0 0 0.1625   0 0 0.1000   1.3
104 RCC 0 0 0.2625   0 0 0.40165  1.42875
105 RCC 0 0 0.66415  0 0 18.23255  2.0726
106 RCC 0 0 0        0 0 19.05    2.225
107 pz 0.160
c ***********************Tissue***********
201 RPP -3.81 3.81 -3.81 3.81 -3.1 -0.01
c ***********************Universe Boundary*************
900 RPP -8 8 -8 8 -15 25

c
c Data Cards
c ************************************************
mode p
c *****NaI************************
m1 11000 -0.1534 53000 -0.8466
c $ NaI (ignoring thallium doping (Hickman))
c
c *****Detector Aluminum window***
m2 13000 1
c
c *****PMT Window*****************
m3 14000 1
c
c *****PMT volume (model as air)
m4 7000 -0.755 8000 -0.232 18000 -0.013
c
c *****Aluminum ******************
m5 13000 1
```

```
c
c *****Dry Air********************
m6 7000 -0.7809 8000 -0.2095 18000 -0.0096
c
c *****Tissue*********************ICRU 44 Adipose
m7     1000 -.114 6000 -.598 7000 -.007 8000 -.278 11000 -.001
       16000 -.001 17000 -.001
C
c ******************Source Definition Cards************
sdef par=2 erg=d1 x=0 y=d2 z=d3
si2 -0.89803 0.89803
sp2 0.0 1.0
si3 -1.816051 -0.02
sp3 0.0 1.0
si1 L 0.01162
     0.013442
     0.013618
     0.0154
     0.015727
     0.01641
     0.016577
     0.017068
     0.017222
     0.017454
     0.020169
     0.020487
     0.020715
     0.020844
     0.093844
     0.094654
     0.098434
     0.110421
     0.111298
     0.111964
     0.114445
     0.114844
sp1 d 0.023110845
     0.038154697
     0.342302136
     0.009157127
     0.006453594
     0.089391004
     0.010029235
     0.018968335
```

```
     0.342302136
     0.009157127
     0.082850199
     0.00414251
     0.003924483
     0.017442147
     0.00000268173
     0.000763094
     0.001242753
     0.000152619
     0.000289976
     0.0000106833
     0.000113374
     0.0000392448
c
c **********************TALLY**************************
c Tally on NAI crystal
f8:p 102
e8 0.0001 95i 0.120 $ 1.252 resolution Energy bins
c FT8 is a Gaussian energy Broadening treatment for tally 8
c a,b,c parameters apply to a nominal NAI(Tl) detector
FT8 GEB -0.0137 0.0752 -0.121
c
c **********************Number of particles***************
nps 50000000
```

Line Source 60° Incident Angle

```
Line Source 60 degree incident angle
c
c Cell Cards
c ***************************************************
c **********************Detector*********************
c *****Aluminum Window***********
101 2 -2.7 -102 imp:p=1
c
c *****NaI Crystal***************
102 1 -3.67 -103 imp:p=1
c
c *****PMT Window****************
103 3 -2.33 -104 imp:p=1
c
c *****PMT Volume****************
104 4 -1.22e-3 -105 imp:p=1
c
```

```
c *****Aluminum Detector Case****
105 5 -2.7 -106 (101 102 103 104 105) imp:p=1
c
c *****Air Below Entrance Window**
120 6 -1.22e-3 -101 imp:p=1
c
c ****Tissue*********************
201 7 -1 -201 imp:p=1
c
c ********************Inside Universe (air)***********
900 6 -1.22e-3 106 201 -900 imp:p=1
c
c ********************Outside Universe***************
903 0 900 imp:p=0

c
c Surface Cards
c ***************************************************
c ***********************Detector********************
101 RCC 0 0 0        0 0 0.1600   1.42875
102 RCC 0 0 0.1600   0 0 0.0025   1.42875
103 RCC 0 0 0.1625   0 0 0.1000   1.3
104 RCC 0 0 0.2625   0 0 0.40165  1.42875
105 RCC 0 0 0.66415  0 0 18.23255  2.0726
106 RCC 0 0 0        0 0 19.05    2.225
107 pz 0.160
c ***********************Tissue***********
201 RPP -3.81 3.81 -3.81 3.81 -3.1 -0.01
c ***********************Universe Boundary*************
900 RPP -8 8 -8 8 -15 25

c
c Data Cards
c ***************************************************
mode p
c *****NaI************************
m1 11000 -0.1534 53000 -0.8466
c $ NaI (ignoring thallium doping (Hickman))
c
c *****Detector Aluminum window***
m2 13000 1
c
c *****PMT Window*****************
m3 14000 1
```

```
c
c *****PMT volume (model as air)
m4 7000 -0.755 8000 -0.232 18000 -0.013
c
c *****Aluminum *****************
m5 13000 1
c
c *****Dry Air*********************
m6 7000 -0.7809 8000 -0.2095 18000 -0.0096
c
c *****Tissue*********************ICRU 44 Adipose
m7     1000 -.114 6000 -.598 7000 -.007 8000 -.278 11000 -.001
       16000 -.001 17000 -.001
C
c ******************Source Definition Cards************
sdef par=2 erg=d1 x=0 y=d2 z=d3
si2 -0.635 0.635
sp2 0.0 1.0
si3 -2.219705 -0.02
sp3 0.0 1.0
si1 L 0.01162
     0.013442
     0.013618
     0.0154
     0.015727
     0.01641
     0.016577
     0.017068
     0.017222
     0.017454
     0.020169
     0.020487
     0.020715
     0.020844
     0.093844
     0.094654
     0.098434
     0.110421
     0.111298
     0.111964
     0.114445
     0.114844
sp1 d 0.023110845
     0.038154697
```

```
     0.342302136
     0.009157127
     0.006453594
     0.089391004
     0.010029235
     0.018968335
     0.342302136
     0.009157127
     0.082850199
     0.00414251
     0.003924483
     0.017442147
     0.00000268173
     0.000763094
     0.001242753
     0.000152619
     0.000289976
     0.0000106833
     0.000113374
     0.0000392448
c
c **********************TALLY**********************
c Tally on NAI crystal
f8:p 102
e8 0.0001 95i 0.120 $ 1.252 resolution Energy bins
c FT8 is a Gaussian energy Broadening treatment for tally 8
c a,b,c parameters apply to a nominal NAI(Tl) detector
FT8 GEB -0.0137 0.0752 -0.121
c
c ********************Number of particles***************
nps 50000000
```

Line Source 90° Incident Angle

```
Line source 90 degree incident angle
c
c Cell Cards
c ************************************************
c **********************Detector********************
c *****Aluminum Window***********
101 2 -2.7 -102 imp:p=1
c
c *****NaI Crystal***************
102 1 -3.67 -103 imp:p=1
c
```

```
c *****PMT Window***************
103 3 -2.33 -104 imp:p=1
c
c *****PMT Volume***************
104 4 -1.22e-3 -105 imp:p=1
c
c *****Aluminum Detector Case****
105 5 -2.7 -106 (101 102 103 104 105) imp:p=1
c
c *****Air Below Entrance Window**
120 6 -1.22e-3 -101 imp:p=1
c
c ****Tissue*********************
201 7 -1 -201 imp:p=1
c
c ********************Inside Universe (air)***********
900 6 -1.22e-3 106 201 -900 imp:p=1
c
c ********************Outside Universe***************
903 0 900 imp:p=0

c
c Surface Cards
c ************************************************
c ***********************Detector********************
101 RCC 0 0 0        0 0 0.1600   1.42875
102 RCC 0 0 0.1600   0 0 0.0025   1.42875
103 RCC 0 0 0.1625   0 0 0.1000   1.3
104 RCC 0 0 0.2625   0 0 0.40165  1.42875
105 RCC 0 0 0.66415  0 0 18.23255  2.0726
106 RCC 0 0 0        0 0 19.05    2.225
107 pz 0.160
c ***********************Tissue***********
201 RPP -3.81 3.81 -3.81 3.81 -3.1 -0.01
c ***********************Universe Boundary*************
900 RPP -8 8 -8 8 -15 25

c
c Data Cards
c ************************************************
mode p
c *****NaI************************
m1 11000 -0.1534 53000 -0.8466
c $ NaI (ignoring thallium doping (Hickman))
```

```
c
c *****Detector Aluminum window***
m2 13000 1
c
c *****PMT Window*****************
m3 14000 1
c
c *****PMT volume (model as air)
m4 7000 -0.755 8000 -0.232 18000 -0.013
c
c *****Aluminum *****************
m5 13000 1
c
c *****Dry Air*******************
m6 7000 -0.7809 8000 -0.2095 18000 -0.0096
c
c *****Tissue*********************ICRU 44 Adipose
m7     1000 -.114 6000 -.598 7000 -.007 8000 -.278 11000 -.001
       16000 -.001 17000 -.001
C
c ******************Source Definition Cards************
sdef par=2 erg=d1 x=0 y=0 z=d3
si3 -2.56 -0.02
sp3 0.0 1.0
si1 L 0.01162
     0.013442
     0.013618
     0.0154
     0.015727
     0.01641
     0.016577
     0.017068
     0.017222
     0.017454
     0.020169
     0.020487
     0.020715
     0.020844
     0.093844
     0.094654
     0.098434
     0.110421
     0.111298
     0.111964
```

```
     0.114445
     0.114844
sp1 d 0.023110845
     0.038154697
     0.342302136
     0.009157127
     0.006453594
     0.089391004
     0.010029235
     0.018968335
     0.342302136
     0.009157127
     0.082850199
     0.00414251
     0.003924483
     0.017442147
     0.00000268173
     0.000763094
     0.001242753
     0.000152619
     0.000289976
     0.0000106833
     0.000113374
     0.0000392448
c
c **********************TALLY*************************
c Tally on NAI crystal
f8:p 102
e8 0.0001 95i 0.120 $ 1.252 resolution Energy bins
c FT8 is a Gaussian energy Broadening treatment for tally 8
c a,b,c parameters apply to a nominal NAI(Tl) detector
FT8 GEB -0.0137 0.0752 -0.121
c
c **********************Number of particles***************
nps 50000000
```

HPGe MCNP INPUT FILES

Point Source 0mm Depth in Tissue

```
Point Source 0mm depth in tissue
c
c Cell cards
c ************Detector**************
101 3 -1.85    -1       imp:p=1
102 2 -1.22e-4 -2       imp:p=1
103 4 -5.323   -3       imp:p=1
104 4 -5.323   -4       imp:p=1
105 5 -2.7     -5 4 3   imp:p=1
106 2 -1.22e-4 -6 5     imp:p=1
107 5 -2.7     -7 6 1 2 imp:p=1
108 5 -2.7     -8       imp:p=1
c Tissue
50  6 -1.0     -50      imp:p=1
c Inside universe
200 1 -1.22e-3  1 2 7 8 50 -900  imp:p=1
c Outside universe
201 0           900     imp:p=0

c Surface Cards
c *************Detector*************
1 RCC 0 0 0        0 -0.0254 0  3.71
2 RCC 0 -0.0254 0  0 -0.5000 0  3.71
3 RCC 0 -0.5254 0  0 -0.0003 0  1.8
4 RCC 0 -0.5257 0  0 -1.3000 0  1.8
5 RCC 0 -0.5254 0  0 -2.3000 0  1.9
6 RCC 0 -0.5254 0  0 -2.3000 0  3.71
7 RCC 0  0      0  0 -2.8258 0  3.81
8 RCC 0 -2.8258 0  0 -0.1000 0  3.81
c ******Tissue******
50 RPP -4 4 0.01 4 -4 4
c *************Universe Boundary*****
900 RPP -10 10 -10 10 -10 10

c Data Cards
mode p
c Dry Air
m1 7000 -0.755 8000 -0.232 18000 -0.013
c Vacuum
m2 7000 -0.755 8000 -0.232 18000 -0.013
c Beryllium
m3 4000 1
```

```
c Germanium
m4 32000 1
c Aluminum
m5 13000 1
c *****Tissue**********ICRU 44 Adipose
m6     1000 -.114 6000 -.598 7000 -.007 8000 -.278 11000 -.001
       16000 -.001 17000 -.001
c
sdef par=2 erg=d2 x=0 y=0.02 z=0
si2 L 0.01162
      0.013442
      0.013618
      0.0154
      0.015727
      0.01641
      0.016577
      0.017068
      0.017222
      0.017454
      0.020169
      0.020487
      0.020715
      0.020844
      0.093844
      0.094654
      0.098434
      0.110421
      0.111298
      0.111964
      0.114445
      0.114844
sp2 d 0.023110845
      0.038154697
      0.342302136
      0.009157127
      0.006453594
      0.089391004
      0.010029235
      0.018968335
      0.342302136
      0.009157127
      0.082850199
      0.00414251
      0.003924483
```

```
     0.017442147
     0.00000268173
     0.000763094
     0.001242753
     0.000152619
     0.000289976
     0.0000106833
     0.000113374
     0.0000392448
c
f8:p 104
e8 0.0001 500i 0.05 $ 0.1 keV resolution Energy bins
c
c **********Number of particles**********
nps 50000000
```

Point Source 2mm Depth in Tissue

```
Point source 2mm depth in tissue
c
c Cell cards
c **********Detector**********
101 3 -1.85    -1       imp:p=1
102 2 -1.22e-4 -2       imp:p=1
103 4 -5.323   -3       imp:p=1
104 4 -5.323   -4       imp:p=1
105 5 -2.7     -5 4 3   imp:p=1
106 2 -1.22e-4 -6 5     imp:p=1
107 5 -2.7     -7 6 1 2 imp:p=1
108 5 -2.7     -8       imp:p=1
c Tissue
50  6 -1.0     -50      imp:p=1
c Inside universe
200 1 -1.22e-3  1 2 7 8 50 -900  imp:p=1
c Outside universe
201 0           900     imp:p=0

c Surface Cards
c **********Detector**********
1 RCC 0 0 0        0 -0.0254 0  3.71
2 RCC 0 -0.0254 0  0 -0.5000 0  3.71
```

```
3 RCC 0 -0.5254 0  0 -0.0003 0  1.8
4 RCC 0 -0.5257 0  0 -1.3000 0  1.8
5 RCC 0 -0.5254 0  0 -2.3000 0  1.9
6 RCC 0 -0.5254 0  0 -2.3000 0  3.71
7 RCC 0  0      0  0 -2.8258 0  3.81
8 RCC 0 -2.8258 0  0 -0.1000 0  3.81
c ******Tissue******
50 RPP -4 4 0.01 4 -4 4
c ************Universe Boundary*****
900 RPP -10 10 -10 10 -10 10

c Data Cards
mode p
c Dry Air
m1 7000 -0.755 8000 -0.232 18000 -0.013
c Vacuum
m2 7000 -0.755 8000 -0.232 18000 -0.013
c Beryllium
m3 4000 1
c Germanium
m4 32000 1
c Aluminum
m5 13000 1
c *****Tissue**********************ICRU 44 Adipose
m6     1000 -.114 6000 -.598 7000 -.007 8000 -.278 11000 -.001
       16000 -.001 17000 -.001
c
sdef par=2 erg=d2 x=0 y=0.22 z=0
si2 L 0.01162
      0.013442
      0.013618
      0.0154
      0.015727
      0.01641
      0.016577
      0.017068
      0.017222
      0.017454
      0.020169
      0.020487
      0.020715
      0.020844
      0.093844
      0.094654
```

```
     0.098434
     0.110421
     0.111298
     0.111964
     0.114445
     0.114844
sp2 d 0.023110845
     0.038154697
     0.342302136
     0.009157127
     0.006453594
     0.089391004
     0.010029235
     0.018968335
     0.342302136
     0.009157127
     0.082850199
     0.00414251
     0.003924483
     0.017442147
     0.00000268173
     0.000763094
     0.001242753
     0.000152619
     0.000289976
     0.0000106833
     0.000113374
     0.0000392448
c
f8:p 104
e8 0.0001 500i 0.05 $ 0.1 keV resolution Energy bins
c
c **********Number of particles**********
nps 50000000
```

Point Source 4mm Depth in Tissue

```
Point source 4mm depth in tissue
c
c Cell cards
c ************Detector**************
101 3 -1.85    -1       imp:p=1
102 2 -1.22e-4 -2       imp:p=1
103 4 -5.323   -3       imp:p=1
104 4 -5.323   -4       imp:p=1
105 5 -2.7     -5 4 3   imp:p=1
106 2 -1.22e-4 -6 5     imp:p=1
107 5 -2.7     -7 6 1 2 imp:p=1
108 5 -2.7     -8       imp:p=1
c Tissue
50  6 -1.0     -50      imp:p=1
c Inside universe
200 1 -1.22e-3  1 2 7 8 50 -900  imp:p=1
c Outside universe
201 0           900     imp:p=0

c Surface Cards
c *************Detector*************
1 RCC 0 0 0        0 -0.0254 0  3.71
2 RCC 0 -0.0254 0  0 -0.5000 0  3.71
3 RCC 0 -0.5254 0  0 -0.0003 0  1.8
4 RCC 0 -0.5257 0  0 -1.3000 0  1.8
5 RCC 0 -0.5254 0  0 -2.3000 0  1.9
6 RCC 0 -0.5254 0  0 -2.3000 0  3.71
7 RCC 0  0      0  0 -2.8258 0  3.81
8 RCC 0 -2.8258 0  0 -0.1000 0  3.81
c ******Tissue******
50 RPP -4 4 0.01 4 -4 4
c *************Universe Boundary*****
900 RPP -10 10 -10 10 -10 10

c Data Cards
mode p
c Dry Air
m1 7000 -0.755 8000 -0.232 18000 -0.013
c Vacuum
m2 7000 -0.755 8000 -0.232 18000 -0.013
c Beryllium
m3 4000 1
c Germanium
m4 32000 1
```

```
c Aluminum
m5 13000 1
c *****Tissue**********ICRU 44 Adipose
m6     1000 -.114 6000 -.598 7000 -.007 8000 -.278 11000 -.001
       16000 -.001 17000 -.001
c
sdef par=2 erg=d2 x=0 y=0.42 z=0
si2 L 0.01162
      0.013442
      0.013618
      0.0154
      0.015727
      0.01641
      0.016577
      0.017068
      0.017222
      0.017454
      0.020169
      0.020487
      0.020715
      0.020844
      0.093844
      0.094654
      0.098434
      0.110421
      0.111298
      0.111964
      0.114445
      0.114844
sp2 d 0.023110845
      0.038154697
      0.342302136
      0.009157127
      0.006453594
      0.089391004
      0.010029235
      0.018968335
      0.342302136
      0.009157127
      0.082850199
      0.00414251
      0.003924483
      0.017442147
      0.00000268173
```

```
     0.000763094
     0.001242753
     0.000152619
     0.000289976
     0.0000106833
     0.000113374
     0.0000392448
c
f8:p 104
e8 0.0001 500i 0.05 $ 0.1 keV resolution Energy bins
c
c **********Number of particles**********
nps 50000000
```

Point Source 6mm Depth in Tissue

```
Point source 6mm depth in tissue
c
c Cell cards
c **********Detector**********
101 3 -1.85    -1       imp:p=1
102 2 -1.22e-4 -2       imp:p=1
103 4 -5.323   -3       imp:p=1
104 4 -5.323   -4       imp:p=1
105 5 -2.7     -5 4 3   imp:p=1
106 2 -1.22e-4 -6 5     imp:p=1
107 5 -2.7     -7 6 1 2 imp:p=1
108 5 -2.7     -8       imp:p=1
c Tissue
50  6 -1.0     -50      imp:p=1
c Inside universe
200 1 -1.22e-3  1 2 7 8 50 -900  imp:p=1
c Outside universe
201 0           900     imp:p=0

c Surface Cards
c **********Detector**********
1 RCC 0 0 0        0 -0.0254 0  3.71
2 RCC 0 -0.0254 0  0 -0.5000 0  3.71
3 RCC 0 -0.5254 0  0 -0.0003 0  1.8
4 RCC 0 -0.5257 0  0 -1.3000 0  1.8
```

```
5 RCC 0 -0.5254 0  0 -2.3000 0  1.9
6 RCC 0 -0.5254 0  0 -2.3000 0  3.71
7 RCC 0  0      0  0 -2.8258 0  3.81
8 RCC 0 -2.8258 0  0 -0.1000 0  3.81
c ******Tissue******
50 RPP -4 4 0.01 4 -4 4
c *************Universe Boundary*****
900 RPP -10 10 -10 10 -10 10

c Data Cards
mode p
c Dry Air
m1 7000 -0.755 8000 -0.232 18000 -0.013
c Vacuum
m2 7000 -0.755 8000 -0.232 18000 -0.013
c Beryllium
m3 4000 1
c Germanium
m4 32000 1
c Aluminum
m5 13000 1
c *****Tissue**********************ICRU 44 Adipose
m6     1000 -.114 6000 -.598 7000 -.007 8000 -.278 11000 -.001
       16000 -.001 17000 -.001
c
sdef par=2 erg=d2 x=0 y=0.62 z=0
si2 L 0.01162
      0.013442
      0.013618
      0.0154
      0.015727
      0.01641
      0.016577
      0.017068
      0.017222
      0.017454
      0.020169
      0.020487
      0.020715
      0.020844
      0.093844
      0.094654
      0.098434
      0.110421
```

```
     0.111298
     0.111964
     0.114445
     0.114844
sp2 d 0.023110845
     0.038154697
     0.342302136
     0.009157127
     0.006453594
     0.089391004
     0.010029235
     0.018968335
     0.342302136
     0.009157127
     0.082850199
     0.00414251
     0.003924483
     0.017442147
     0.00000268173
     0.000763094
     0.001242753
     0.000152619
     0.000289976
     0.0000106833
     0.000113374
     0.0000392448
c
f8:p 104
e8 0.0001 500i 0.05 $ 0.1 keV resolution Energy bins
c
c **********Number of particles**********
nps 50000000
```

Point Source 10mm Depth in Tissue

```
Point source 10mm depth in tissue
c
c Cell cards
c ************Detector**************
101 3 -1.85    -1       imp:p=1
102 2 -1.22e-4 -2       imp:p=1
103 4 -5.323   -3       imp:p=1
104 4 -5.323   -4       imp:p=1
105 5 -2.7     -5 4 3   imp:p=1
106 2 -1.22e-4 -6 5     imp:p=1
107 5 -2.7     -7 6 1 2 imp:p=1
108 5 -2.7     -8       imp:p=1
c Tissue
50  6 -1.0     -50      imp:p=1
c Inside universe
200 1 -1.22e-3  1 2 7 8 50 -900  imp:p=1
c Outside universe
201 0           900     imp:p=0

c Surface Cards
c *************Detector*************
1 RCC 0 0 0        0 -0.0254 0  3.71
2 RCC 0 -0.0254 0  0 -0.5000 0  3.71
3 RCC 0 -0.5254 0  0 -0.0003 0  1.8
4 RCC 0 -0.5257 0  0 -1.3000 0  1.8
5 RCC 0 -0.5254 0  0 -2.3000 0  1.9
6 RCC 0 -0.5254 0  0 -2.3000 0  3.71
7 RCC 0  0      0  0 -2.8258 0  3.81
8 RCC 0 -2.8258 0  0 -0.1000 0  3.81
c ******Tissue******
50 RPP -4 4 0.01 4 -4 4
c *************Universe Boundary*****
900 RPP -10 10 -10 10 -10 10

c Data Cards
mode p
c Dry Air
m1 7000 -0.755 8000 -0.232 18000 -0.013
c Vacuum
m2 7000 -0.755 8000 -0.232 18000 -0.013
c Beryllium
m3 4000 1
c Germanium
m4 32000 1
```

```
c Aluminum
m5 13000 1
c *****Tissue**********ICRU 44 Adipose
m6     1000 -.114 6000 -.598 7000 -.007 8000 -.278 11000 -.001
       16000 -.001 17000 -.001
c
sdef par=2 erg=d2 x=0 y=1.02 z=0
si2 L 0.01162
      0.013442
      0.013618
      0.0154
      0.015727
      0.01641
      0.016577
      0.017068
      0.017222
      0.017454
      0.020169
      0.020487
      0.020715
      0.020844
      0.093844
      0.094654
      0.098434
      0.110421
      0.111298
      0.111964
      0.114445
      0.114844
sp2 d 0.023110845
      0.038154697
      0.342302136
      0.009157127
      0.006453594
      0.089391004
      0.010029235
      0.018968335
      0.342302136
      0.009157127
      0.082850199
      0.00414251
      0.003924483
      0.017442147
      0.00000268173
```

```
     0.000763094
     0.001242753
     0.000152619
     0.000289976
     0.0000106833
     0.000113374
     0.0000392448
c
f8:p 104
e8 0.0001 500i 0.05 $ 0.1 keV resolution Energy bins
c
c **********Number of particles**********
nps 50000000
```

Point Source 15mm Depth in Tissue

```
Point source 15mm depth in tissue
c
c Cell cards
c **********Detector**********
101 3 -1.85    -1       imp:p=1
102 2 -1.22e-4 -2       imp:p=1
103 4 -5.323   -3       imp:p=1
104 4 -5.323   -4       imp:p=1
105 5 -2.7     -5 4 3   imp:p=1
106 2 -1.22e-4 -6 5     imp:p=1
107 5 -2.7     -7 6 1 2 imp:p=1
108 5 -2.7     -8       imp:p=1
c Tissue
50  6 -1.0     -50      imp:p=1
c Inside universe
200 1 -1.22e-3  1 2 7 8 50 -900  imp:p=1
c Outside universe
201 0           900     imp:p=0

c Surface Cards
c **********Detector**********
1 RCC 0 0 0        0 -0.0254 0  3.71
2 RCC 0 -0.0254 0  0 -0.5000 0  3.71
3 RCC 0 -0.5254 0  0 -0.0003 0  1.8
4 RCC 0 -0.5257 0  0 -1.3000 0  1.8
```

```
5 RCC 0 -0.5254 0  0 -2.3000 0  1.9
6 RCC 0 -0.5254 0  0 -2.3000 0  3.71
7 RCC 0  0      0  0 -2.8258 0  3.81
8 RCC 0 -2.8258 0  0 -0.1000 0  3.81
c ******Tissue******
50 RPP -4 4 0.01 4 -4 4
c *************Universe Boundary*****
900 RPP -10 10 -10 10 -10 10

c Data Cards
mode p
c Dry Air
m1 7000 -0.755 8000 -0.232 18000 -0.013
c Vacuum
m2 7000 -0.755 8000 -0.232 18000 -0.013
c Beryllium
m3 4000 1
c Germanium
m4 32000 1
c Aluminum
m5 13000 1
c *****Tissue**********************ICRU 44 Adipose
m6     1000 -.114 6000 -.598 7000 -.007 8000 -.278 11000 -.001
       16000 -.001 17000 -.001
c
sdef par=2 erg=d2 x=0 y=1.52 z=0
si2 L 0.01162
      0.013442
      0.013618
      0.0154
      0.015727
      0.01641
      0.016577
      0.017068
      0.017222
      0.017454
      0.020169
      0.020487
      0.020715
      0.020844
      0.093844
      0.094654
      0.098434
      0.110421
```

```
     0.111298
     0.111964
     0.114445
     0.114844
sp2 d 0.023110845
     0.038154697
     0.342302136
     0.009157127
     0.006453594
     0.089391004
     0.010029235
     0.018968335
     0.342302136
     0.009157127
     0.082850199
     0.00414251
     0.003924483
     0.017442147
     0.00000268173
     0.000763094
     0.001242753
     0.000152619
     0.000289976
     0.0000106833
     0.000113374
     0.0000392448
c
f8:p 104
e8 0.0001 500i 0.05 $ 0.1 keV resolution Energy bins
c
c **********Number of particles**********
nps 50000000
```

Point Source 20mm Depth in Tissue

```
Point source 20mm depth in tissue
c
c Cell cards
c ************Detector**************
101 3 -1.85    -1       imp:p=1
102 2 -1.22e-4 -2       imp:p=1
103 4 -5.323   -3       imp:p=1
104 4 -5.323   -4       imp:p=1
105 5 -2.7     -5 4 3   imp:p=1
106 2 -1.22e-4 -6 5     imp:p=1
107 5 -2.7     -7 6 1 2 imp:p=1
108 5 -2.7     -8       imp:p=1
c Tissue
50  6 -1.0     -50      imp:p=1
c Inside universe
200 1 -1.22e-3  1 2 7 8 50 -900  imp:p=1
c Outside universe
201 0           900     imp:p=0

c Surface Cards
c *************Detector*************
1 RCC 0 0 0        0 -0.0254 0  3.71
2 RCC 0 -0.0254 0  0 -0.5000 0  3.71
3 RCC 0 -0.5254 0  0 -0.0003 0  1.8
4 RCC 0 -0.5257 0  0 -1.3000 0  1.8
5 RCC 0 -0.5254 0  0 -2.3000 0  1.9
6 RCC 0 -0.5254 0  0 -2.3000 0  3.71
7 RCC 0  0      0  0 -2.8258 0  3.81
8 RCC 0 -2.8258 0  0 -0.1000 0  3.81
c ******Tissue******
50 RPP -4 4 0.01 4 -4 4
c *************Universe Boundary*****
900 RPP -10 10 -10 10 -10 10

c Data Cards
mode p
c Dry Air
m1 7000 -0.755 8000 -0.232 18000 -0.013
c Vacuum
m2 7000 -0.755 8000 -0.232 18000 -0.013
c Beryllium
m3 4000 1
c Germanium
m4 32000 1
```

```
c Aluminum
m5 13000 1
c *****Tissue**********ICRU 44 Adipose
m6     1000 -.114 6000 -.598 7000 -.007 8000 -.278 11000 -.001
       16000 -.001 17000 -.001
c
sdef par=2 erg=d2 x=0 y=2.02 z=0
si2 L 0.01162
      0.013442
      0.013618
      0.0154
      0.015727
      0.01641
      0.016577
      0.017068
      0.017222
      0.017454
      0.020169
      0.020487
      0.020715
      0.020844
      0.093844
      0.094654
      0.098434
      0.110421
      0.111298
      0.111964
      0.114445
      0.114844
sp2 d 0.023110845
      0.038154697
      0.342302136
      0.009157127
      0.006453594
      0.089391004
      0.010029235
      0.018968335
      0.342302136
      0.009157127
      0.082850199
      0.00414251
      0.003924483
      0.017442147
      0.00000268173
```

```
     0.000763094
     0.001242753
     0.000152619
     0.000289976
     0.0000106833
     0.000113374
     0.0000392448
c
f8:p 104
e8 0.0001 500i 0.05 $ 0.1 keV resolution Energy bins
c
c **********Number of particles**********
nps 50000000
```

Line Source 0° Incident Angle

```
HPGe Simple Geometry
c
c Cell cards
c **********Detector**********
101 3 -1.85    -1       imp:p=1
102 2 -1.22e-4 -2       imp:p=1
103 4 -5.323   -3       imp:p=1
104 4 -5.323   -4       imp:p=1
105 5 -2.7     -5 4 3   imp:p=1
106 2 -1.22e-4 -6 5     imp:p=1
107 5 -2.7     -7 6 1 2 imp:p=1
108 5 -2.7     -8       imp:p=1
c Tissue
50  6 -1.0     -50      imp:p=1
c Inside universe
200 1 -1.22e-3  1 2 7 8 50 -900  imp:p=1
c Outside universe
201 0           900     imp:p=0

c Surface Cards
c **********Detector**********
1 RCC 0 0 0        0 -0.0254 0  3.71
2 RCC 0 -0.0254 0  0 -0.5000 0  3.71
3 RCC 0 -0.5254 0  0 -0.0003 0  1.8
4 RCC 0 -0.5257 0  0 -1.3000 0  1.8
```

```
5 RCC 0 -0.5254 0  0 -2.3000 0  1.9
6 RCC 0 -0.5254 0  0 -2.3000 0  3.71
7 RCC 0  0      0  0 -2.8258 0  3.81
8 RCC 0 -2.8258 0  0 -0.1000 0  3.81
c ******Tissue******
50 RPP -4 4 0.01 4 -4 4
c *************Universe Boundary*****
900 RPP -10 10 -10 10 -10 10

c Data Cards
mode p
c Dry Air
m1 7000 -0.755 8000 -0.232 18000 -0.013
c Vacuum
m2 7000 -0.755 8000 -0.232 18000 -0.013
c Beryllium
m3 4000 1
c Germanium
m4 32000 1
c Aluminum
m5 13000 1
c *****Tissue**********************ICRU 44 Adipose
m6     1000 -.114 6000 -.598 7000 -.007 8000 -.278 11000 -.001
       16000 -.001 17000 -.001
c
sdef par=2 erg=d2 x=0 y=0.02 z=d1
si1 -1.27 1.27
sp1  0.0 1.0
si2 L 0.01162
      0.013442
      0.013618
      0.0154
      0.015727
      0.01641
      0.016577
      0.017068
      0.017222
      0.017454
      0.020169
      0.020487
      0.020715
      0.020844
      0.093844
      0.094654
```

```
     0.098434
     0.110421
     0.111298
     0.111964
     0.114445
     0.114844
sp2 d 0.023110845
     0.038154697
     0.342302136
     0.009157127
     0.006453594
     0.089391004
     0.010029235
     0.018968335
     0.342302136
     0.009157127
     0.082850199
     0.00414251
     0.003924483
     0.017442147
     0.00000268173
     0.000763094
     0.001242753
     0.000152619
     0.000289976
     0.0000106833
     0.000113374
     0.0000392448
c
f8:p 104
e8 0.0001 500i 0.05 $ 0.1 keV resolution Energy bins
c
c **********Number of particles**********
nps 50000000
```

Line Source 15° Incident Angle

```
HPGe Simple Geometry
c
c Cell cards
c ************Detector**************
101 3 -1.85    -1       imp:p=1
102 2 -1.22e-4 -2       imp:p=1
103 4 -5.323   -3       imp:p=1
104 4 -5.323   -4       imp:p=1
105 5 -2.7     -5 4 3   imp:p=1
106 2 -1.22e-4 -6 5     imp:p=1
107 5 -2.7     -7 6 1 2 imp:p=1
108 5 -2.7     -8       imp:p=1
c Tissue
50  6 -1.0     -50      imp:p=1
c Inside universe
200 1 -1.22e-3  1 2 7 8 50 -900  imp:p=1
c Outside universe
201 0           900     imp:p=0

c Surface Cards
c *************Detector*************
1 RCC 0 0 0        0 -0.0254 0  3.71
2 RCC 0 -0.0254 0  0 -0.5000 0  3.71
3 RCC 0 -0.5254 0  0 -0.0003 0  1.8
4 RCC 0 -0.5257 0  0 -1.3000 0  1.8
5 RCC 0 -0.5254 0  0 -2.3000 0  1.9
6 RCC 0 -0.5254 0  0 -2.3000 0  3.71
7 RCC 0  0      0  0 -2.8258 0  3.81
8 RCC 0 -2.8258 0  0 -0.1000 0  3.81
c ******Tissue******
50 RPP -4 4 0.01 4 -4 4
c *************Universe Boundary*****
900 RPP -10 10 -10 10 -10 10

c Data Cards
mode p
c Dry Air
m1 7000 -0.755 8000 -0.232 18000 -0.013
c Vacuum
m2 7000 -0.755 8000 -0.232 18000 -0.013
c Beryllium
m3 4000 1
c Germanium
m4 32000 1
```

```
c Aluminum
m5 13000 1
c *****Tissue**********ICRU 44 Adipose
m6     1000 -.114 6000 -.598 7000 -.007 8000 -.278 11000 -.001
       16000 -.001 17000 -.001
c
sdef par=2 erg=d2 x=0 y=d1 z=d3
si1  0.02 0.6774
sp1  0.0 1.0
si3 -1.226726 1.226726
sp3  0.0 1.0
si2 L 0.01162
      0.013442
      0.013618
      0.0154
      0.015727
      0.01641
      0.016577
      0.017068
      0.017222
      0.017454
      0.020169
      0.020487
      0.020715
      0.020844
      0.093844
      0.094654
      0.098434
      0.110421
      0.111298
      0.111964
      0.114445
      0.114844
sp2 d 0.023110845
      0.038154697
      0.342302136
      0.009157127
      0.006453594
      0.089391004
      0.010029235
      0.018968335
      0.342302136
      0.009157127
      0.082850199
```

```
     0.00414251
     0.003924483
     0.017442147
     0.00000268173
     0.000763094
     0.001242753
     0.000152619
     0.000289976
     0.0000106833
     0.000113374
     0.0000392448
c
f8:p 104
e8 0.0001 500i 0.05 $ 0.1 keV resolution Energy bins
c
c **********Number of particles**********
nps 50000000
```

Line Source 30° Incident Angle

```
HPGe Simple Geometry
c
c Cell cards
c **********Detector**********
101 3 -1.85    -1       imp:p=1
102 2 -1.22e-4 -2       imp:p=1
103 4 -5.323   -3       imp:p=1
104 4 -5.323   -4       imp:p=1
105 5 -2.7     -5 4 3   imp:p=1
106 2 -1.22e-4 -6 5     imp:p=1
107 5 -2.7     -7 6 1 2 imp:p=1
108 5 -2.7     -8       imp:p=1
c Tissue
50  6 -1.0     -50      imp:p=1
c Inside universe
200 1 -1.22e-3  1 2 7 8 50 -900  imp:p=1
c Outside universe
201 0           900     imp:p=0

c Surface Cards
c **********Detector**********
```

```
1 RCC 0 0 0        0 -0.0254 0  3.71
2 RCC 0 -0.0254 0  0 -0.5000 0  3.71
3 RCC 0 -0.5254 0  0 -0.0003 0  1.8
4 RCC 0 -0.5257 0  0 -1.3000 0  1.8
5 RCC 0 -0.5254 0  0 -2.3000 0  1.9
6 RCC 0 -0.5254 0  0 -2.3000 0  3.71
7 RCC 0  0      0  0 -2.8258 0  3.81
8 RCC 0 -2.8258 0  0 -0.1000 0  3.81
c ******Tissue******
50 RPP -4 4 0.01 4 -4 4
c *************Universe Boundary*****
900 RPP -10 10 -10 10 -10 10

c Data Cards
mode p
c Dry Air
m1 7000 -0.755 8000 -0.232 18000 -0.013
c Vacuum
m2 7000 -0.755 8000 -0.232 18000 -0.013
c Beryllium
m3 4000 1
c Germanium
m4 32000 1
c Aluminum
m5 13000 1
c *****Tissue**********************ICRU 44 Adipose
m6     1000 -.114 6000 -.598 7000 -.007 8000 -.278 11000 -.001
       16000 -.001 17000 -.001
c
sdef par=2 erg=d2 x=0 y=d1 z=d3
si1  0.02 1.29
sp1  0.0 1.0
si3 -1.09985 1.09985
sp3  0.0 1.0
si2 L 0.01162
      0.013442
      0.013618
      0.0154
      0.015727
      0.01641
      0.016577
      0.017068
      0.017222
      0.017454
```

```
     0.020169
     0.020487
     0.020715
     0.020844
     0.093844
     0.094654
     0.098434
     0.110421
     0.111298
     0.111964
     0.114445
     0.114844
sp2 d 0.023110845
     0.038154697
     0.342302136
     0.009157127
     0.006453594
     0.089391004
     0.010029235
     0.018968335
     0.342302136
     0.009157127
     0.082850199
     0.00414251
     0.003924483
     0.017442147
     0.00000268173
     0.000763094
     0.001242753
     0.000152619
     0.000289976
     0.0000106833
     0.000113374
     0.0000392448
c
f8:p 104
e8 0.0001 500i 0.05 $ 0.1 keV resolution Energy bins
c
c **********Number of particles**********
nps 50000000
```

Line Source 45° Incident Angle

```
HPGe Simple Geometry
c
c Cell cards
c ************Detector**************
101 3 -1.85    -1       imp:p=1
102 2 -1.22e-4 -2       imp:p=1
103 4 -5.323   -3       imp:p=1
104 4 -5.323   -4       imp:p=1
105 5 -2.7     -5 4 3   imp:p=1
106 2 -1.22e-4 -6 5     imp:p=1
107 5 -2.7     -7 6 1 2 imp:p=1
108 5 -2.7     -8       imp:p=1
c Tissue
50  6 -1.0     -50      imp:p=1
c Inside universe
200 1 -1.22e-3  1 2 7 8 50 -900  imp:p=1
c Outside universe
201 0           900     imp:p=0

c Surface Cards
c *************Detector*************
1 RCC 0 0 0        0 -0.0254 0  3.71
2 RCC 0 -0.0254 0  0 -0.5000 0  3.71
3 RCC 0 -0.5254 0  0 -0.0003 0  1.8
4 RCC 0 -0.5257 0  0 -1.3000 0  1.8
5 RCC 0 -0.5254 0  0 -2.3000 0  1.9
6 RCC 0 -0.5254 0  0 -2.3000 0  3.71
7 RCC 0  0      0  0 -2.8258 0  3.81
8 RCC 0 -2.8258 0  0 -0.1000 0  3.81
c ******Tissue******
50 RPP -4 4 0.01 4 -4 4
c *************Universe Boundary*****
900 RPP -10 10 -10 10 -10 10

c Data Cards
mode p
c Dry Air
m1 7000 -0.755 8000 -0.232 18000 -0.013
c Vacuum
m2 7000 -0.755 8000 -0.232 18000 -0.013
c Beryllium
m3 4000 1
c Germanium
m4 32000 1
```

```
c Aluminum
m5 13000 1
c *****Tissue**********************ICRU 44 Adipose
m6     1000 -.114 6000 -.598 7000 -.007 8000 -.278 11000 -.001
       16000 -.001 17000 -.001
c
sdef par=2 erg=d2 x=0 y=d1 z=d3
si1  0.02 1.816051
sp1  0.0 1.0
si3 -0.89803 0.89803
sp3  0.0 1.0
si2 L 0.01162
      0.013442
      0.013618
      0.0154
      0.015727
      0.01641
      0.016577
      0.017068
      0.017222
      0.017454
      0.020169
      0.020487
      0.020715
      0.020844
      0.093844
      0.094654
      0.098434
      0.110421
      0.111298
      0.111964
      0.114445
      0.114844
sp2 d 0.023110845
      0.038154697
      0.342302136
      0.009157127
      0.006453594
      0.089391004
      0.010029235
      0.018968335
      0.342302136
      0.009157127
      0.082850199
```

```
     0.00414251
     0.003924483
     0.017442147
     0.00000268173
     0.000763094
     0.001242753
     0.000152619
     0.000289976
     0.0000106833
     0.000113374
     0.0000392448
c
f8:p 104
e8 0.0001 500i 0.05 $ 0.1 keV resolution Energy bins
c
c **********Number of particles**********
nps 50000000
```

Line Source 60° Incident Angle

```
HPGe Simple Geometry
c
c Cell cards
c **********Detector**********
101 3 -1.85    -1       imp:p=1
102 2 -1.22e-4 -2       imp:p=1
103 4 -5.323   -3       imp:p=1
104 4 -5.323   -4       imp:p=1
105 5 -2.7     -5 4 3   imp:p=1
106 2 -1.22e-4 -6 5     imp:p=1
107 5 -2.7     -7 6 1 2 imp:p=1
108 5 -2.7     -8       imp:p=1
c Tissue
50  6 -1.0     -50      imp:p=1
c Inside universe
200 1 -1.22e-3  1 2 7 8 50 -900  imp:p=1
c Outside universe
201 0           900     imp:p=0

c Surface Cards
c **********Detector**********
```

```
1 RCC 0 0 0        0 -0.0254 0  3.71
2 RCC 0 -0.0254 0  0 -0.5000 0  3.71
3 RCC 0 -0.5254 0  0 -0.0003 0  1.8
4 RCC 0 -0.5257 0  0 -1.3000 0  1.8
5 RCC 0 -0.5254 0  0 -2.3000 0  1.9
6 RCC 0 -0.5254 0  0 -2.3000 0  3.71
7 RCC 0  0      0  0 -2.8258 0  3.81
8 RCC 0 -2.8258 0  0 -0.1000 0  3.81
c ******Tissue******
50 RPP -4 4 0.01 4 -4 4
c *************Universe Boundary*****
900 RPP -10 10 -10 10 -10 10

c Data Cards
mode p
c Dry Air
m1 7000 -0.755 8000 -0.232 18000 -0.013
c Vacuum
m2 7000 -0.755 8000 -0.232 18000 -0.013
c Beryllium
m3 4000 1
c Germanium
m4 32000 1
c Aluminum
m5 13000 1
c *****Tissue**********************ICRU 44 Adipose
m6     1000 -.114 6000 -.598 7000 -.007 8000 -.278 11000 -.001
       16000 -.001 17000 -.001
c
sdef par=2 erg=d2 x=0 y=d1 z=d3
si1  0.02 2.219705
sp1  0.0 1.0
si3 -0.635 0.635
sp3  0.0 1.0
si2 L 0.01162
      0.013442
      0.013618
      0.0154
      0.015727
      0.01641
      0.016577
      0.017068
      0.017222
      0.017454
```

```
     0.020169
     0.020487
     0.020715
     0.020844
     0.093844
     0.094654
     0.098434
     0.110421
     0.111298
     0.111964
     0.114445
     0.114844
sp2 d 0.023110845
     0.038154697
     0.342302136
     0.009157127
     0.006453594
     0.089391004
     0.010029235
     0.018968335
     0.342302136
     0.009157127
     0.082850199
     0.00414251
     0.003924483
     0.017442147
     0.00000268173
     0.000763094
     0.001242753
     0.000152619
     0.000289976
     0.0000106833
     0.000113374
     0.0000392448
c
f8:p 104
e8 0.0001 500i 0.05 $ 0.1 keV resolution Energy bins
c
c **********Number of particles**********
nps 50000000
```

Line Source 90° Incident Angle

```
HPGe Simple Geometry
c
c Cell cards
c ************Detector**************
101 3 -1.85    -1       imp:p=1
102 2 -1.22e-4 -2       imp:p=1
103 4 -5.323   -3       imp:p=1
104 4 -5.323   -4       imp:p=1
105 5 -2.7     -5 4 3   imp:p=1
106 2 -1.22e-4 -6 5     imp:p=1
107 5 -2.7     -7 6 1 2 imp:p=1
108 5 -2.7     -8       imp:p=1
c Tissue
50  6 -1.0     -50      imp:p=1
c Inside universe
200 1 -1.22e-3  1 2 7 8 50 -900  imp:p=1
c Outside universe
201 0           900     imp:p=0

c Surface Cards
c *************Detector*************
1 RCC 0 0 0        0 -0.0254 0  3.71
2 RCC 0 -0.0254 0  0 -0.5000 0  3.71
3 RCC 0 -0.5254 0  0 -0.0003 0  1.8
4 RCC 0 -0.5257 0  0 -1.3000 0  1.8
5 RCC 0 -0.5254 0  0 -2.3000 0  1.9
6 RCC 0 -0.5254 0  0 -2.3000 0  3.71
7 RCC 0  0      0  0 -2.8258 0  3.81
8 RCC 0 -2.8258 0  0 -0.1000 0  3.81
c ******Tissue******
50 RPP -4 4 0.01 4 -4 4
c *************Universe Boundary*****
900 RPP -10 10 -10 10 -10 10

c Data Cards
mode p
c Dry Air
m1 7000 -0.755 8000 -0.232 18000 -0.013
c Vacuum
m2 7000 -0.755 8000 -0.232 18000 -0.013
c Beryllium
m3 4000 1
c Germanium
```

```
m4 32000 1
c Aluminum
m5 13000 1
c *****Tissue**********ICRU 44 Adipose
m6     1000 -.114 6000 -.598 7000 -.007 8000 -.278 11000 -.001
       16000 -.001 17000 -.001
c
sdef par=2 erg=d2 x=0 y=d1 z=0
si1  0.02 2.56
sp1  0.0 1.0
si2 L 0.01162
      0.013442
      0.013618
      0.0154
      0.015727
      0.01641
      0.016577
      0.017068
      0.017222
      0.017454
      0.020169
      0.020487
      0.020715
      0.020844
      0.093844
      0.094654
      0.098434
      0.110421
      0.111298
      0.111964
      0.114445
      0.114844
sp2 d 0.023110845
      0.038154697
      0.342302136
      0.009157127
      0.006453594
      0.089391004
      0.010029235
      0.018968335
      0.342302136
      0.009157127
      0.082850199
      0.00414251
```

```
     0.003924483
     0.017442147
     0.00000268173
     0.000763094
     0.001242753
     0.000152619
     0.000289976
     0.0000106833
     0.000113374
     0.0000392448
c
f8:p 104
e8 0.0001 500i 0.05 $ 0.1 keV resolution Energy bins
c
c **********Number of particles**********
nps 50000000
```

VITA

Name: Paul James Dimmerling

Address: Department of Nuclear Engineering
Texas A&M University
3133 TAMU
College Station, TX 77843-3133

Email Address: paul.dimmerling@gmail.com

Education: B.S., Mechanical Engineering, The Ohio State University, 2005
M.S., Health Physics, Texas A&M University, 2007